Localized Treatment of Malignant Melanoma Using a Modified Cellulose-Based Hydrogel Loaded with Temozolomide with Increased Safety of Human Dermal Fibroblasts and the Mechanisms Behind the Effect

By
Joseph Wolf

Presented to the Faculty of the Graduate School of
The University of Texas at Arlington
in partial fulfillment of the requirements for the degree of
DOCTOR OF PHILOSOPHY

THE UNIVERSITY OF TEXAS AT ARLINGTON
August 2021

Advisor: Dr. Young-Tae Kim

Committee Members:

Dr. Young-Tae Kim, Supervising Professor

Dr. Young-Soo Seo

Dr. Kytai Nguyen

Dr. Georgios Alexandrakis

Dr. Mark Pellegrino

Acknowledgements

It takes a village to raise a child and it definitely took several people to get me through and achieve my doctoral degree. So many people brought specific benefits to assist me, and I am truly thankful. I would like to acknowledge and express my sincere gratitude to Dr. Young-Tae Kim for his continued guidance as my mentor and his ability to push me towards my goals even when I got discouraged. He allowed me to try out different ideas and did not give up on me even when my ideas did not turn out the way we wanted. I would also like to thank Dr. Kytai Nguyen for allowing me the opportunity to work in her lab when I first came to UTA. Her idea to have Linda mentor me as a first year PhD really allowed me to start off on the right foot. I learned so much in her lab that I was able to carry throughout the entirety of my PhD. I would like to thank Dr. Georgios Alexandrakis who I got to know while being his teaching assistant for multiple semesters and as someone who was always available when I had questions. I would like to express my gratitude to all my fellow students who I worked with in the labs I was a part of. I was always welcoming to the advice you gave me, and I appreciate all of it. A few that really went above and beyond to assist me include Victoria Messerschmidt, Linda Noukeu, Roshni Iyer, and Shen Qionghua. Finally, I would like to acknowledge the staff of the Bioengineering department. They greatly assisted me in ensuring I always had a means of support by granting me TA positions every semester and award nominations. Lastly to all my friends that provided the good times, thank you for the temporary escape from experiments and data analysis, specifically Sara Mcmahan, Tyrell Pruitt, Alan Taylor, and Adam Germain.

Dedication

I would like to dedicate this thesis to my late stepmother Jerri Wolf, my father Thomas Wolf, and mother Kathleen Barnes-Evans. They supported me throughout my entire education, and I can definitively say that I would not have been able to complete my degree without them being there for me. This degree is as much theirs as it is mine.

List of Figures

List of Tables

Abstract

Melanoma pathophysiology is highly varied, and the initial cause of tumorigenesis is still unknown, but it is likely a combination of both epigenetic and genetic means. Further, melanoma tumors have one of the highest mutational burdens of all cancers and are largely composed of varied subpopulations within the same tumor. These two factors provide insight into why melanoma is so difficult to treat medicinally. Dacarbazine is the gold-standard of metastatic melanoma treatment, yet only has an overall response rate of 22% and no impact on survival. Temozolomide (TMZ), an analog of dacarbazine, is often viewed as a more ideal choice because of its more favorable side effect profile and its ability to pass across the blood-brain barrier. While Dacarbazine is converted to its active form in the liver, TMZ is converted in the presence of physiological (neutral) pH levels. Local delivery using hydrogels loaded with a specific chemotherapy drug are viewed as a more efficient and safer method of chemotherapy administration. Hydrogels can allow for lower dosages, sustained release, and minimized side-effects to healthy tissue. **The ultimate goal is first to improve the effectiveness of TMZ cytotoxicity in melanoma while being safer to normal skin cells by using a modified cellulose-based hydrogel as a vehicle for drug delivery and second, use the expression of proteins associated with chemoresistance to determine the mechanisms that are overcome by localized sustained delivery.** This is to be accomplished with the use of a hydrogel made of cellulose nano-fibers (CNF) modified with polyacrylic acid (PAA) to retain an acidic environment to prolong TMZ stability and release. Protein analysis of biomolecules that promote chemoresistance will also be analyzed between melanoma and normal cells to better understand by what mechanism hydrogel loaded drug release is more efficient on melanoma cytotoxicity, while simultaneously being safer on normal cells. The strategy to reach the goal of

an improved delivery of TMZ will be accomplished throughout the following aims: **(1)** Determine cell viability of highly resistant Duke melanoma 6 cells (DM6) and human dermal fibroblasts (HDF-α) after treatment with free TMZ and hydrogel delivered TMZ, as well as characterizing the release profile and stability of TMZ when loaded into modified CNF; **(2)** Bridge the gap between in vitro and in vivo using a 3D collagen matrix seeded with DM6 or HDF-α. TMZ delivered via CNF (CNF/TMZ) will be injected in an intratumoral fashion into the gel. **(3)** Protein levels associated with methylated DNA repair and glutathione synthesis, amino acid import, and endogenous cysteine production will be measured to further specify the means CNF/TMZ is able to bypass chemoresistance of DM6 without significant harm to HDF-α. Further analysis will include quantification of oxidative stress molecules and glutathione synthesis specific molecules.

Table of Contents

Chapter 1: Introduction

1.1 Melanoma Epidemiology

Globally skin cancer cases are rising and in 2018 there were a reported 1,325,779 total skin cancer cases, with melanoma of the skin making up 287,723 of the cases. Among skin cancer types melanoma has the highest death amount, with 48.2% of total skin cancer deaths being caused by melanoma [1]. The CDC provides melanoma of the skin statistics from 2009-2017 and the trend shows that the number of new cases continues to rise each year significantly, while deaths for early stages decrease. Annual rates of new cases have increased from 1999-2017 (15.2 – 22.7 per 100,000 people). 2017 had a reported 85,686 cases of melanoma of the skin according to the CDC and case density in 2017 was primarily confined to mid-northern and north-western states, as well as a pocket of south-eastern states, with Florida having the highest incident amount of 7,095 cases. Annual rates of melanoma deaths from 1999-2013 stayed relatively equal (2.6 – 2.7 per 100,000 people, peaking at 2.8 in 2009), until dipping from 2014-2017 (2.6-2.1 per 100,000 people). 2017 reported 8,056 deaths from melanoma, dropping from a peak of 9,394 deaths in 2013 [2]. Melanoma is a cancer that primarily affects those 45 years and older, with a median age of diagnosis of 65. 24.8% of new cases are diagnosed in individuals ranging from 65-74 years old, the highest for any age category provided. Concurrently the highest percentage of deaths due to melanoma occur in the age range of 65-74, with a median age of death being 71 years old [3].

Estimated cases for 2020 are expected to be 100,350, an increase of almost 15,000 cases from 2017 and estimated deaths equaling 6,850, a drop of about 1,200 deaths from 2017. Most of these cases and deaths will occur in Caucasian males, followed by Caucasian females. Based on 2020 estimated new cases, melanoma will represent 5.6% of all new cancer cases in the United States [4]

1.2 Causes and Pathophysiology of Melanoma

Melanocytes are the cells responsible for production of melanin for protection against UV radiation. Melanoma cells are derived from melanocytes, yet the exact mechanics that promote tumorigenesis are still not fully understood. Transformation is likely the result of complex interactions involving both exogenous and endogenous means that could follow a sequential genetic modelling. The result being constitutive activation of several oncogenes. Intermediate lesions and melanomas in situ require mutations such as in telomerase reverse transcriptase (TERT) promoter. Melanomas are highly malignant and tertiary mutations in cell-cycle controlling genes such as cyclin-dependent kinase-inhibitor 2A (CDKN2A) are commonly required. Further metastasis is associated with mutations in phosphatase-and-tensin homologue (PTEN) [5, 6]. These mutations result in overstimulation of several cellular pathways at the protein level, including primarily mitogen-activated-protein-kinase (MAPK) pathway and the phosphoinositide-3-kinase (PI3K) [7].

Of the four major forms of melanoma; superficial spreading, nodular, lentigo maligna, and acral lentiginous melanomas, superficial spreading accounts for about 70% of melanomas. Highest risk factors for melanoma include ultraviolet radiation exposure and subsequent sunburns. Epidemiological and molecular data provide a claim for two definite aetiological mechanisms as to how UV radiation increases melanoma tumorigenesis. Intermittent sun exposure and early in life sun exposure tend to promote a B-Raf proto-oncogene serine/threonine-kinase (BRAF)-associated pathway. Overtime, accumulated sun exposure leads to NRAS proto-oncogene GTPase (NRAS) mutations, a so-called chronic sun exposure pathway. UV radiation exposure leads to DNA mutations such as the formation of pyrimidine dimers or deamination of cytosine into thymidine. UV mutagenic effects are associated with the much higher base mutation rate seen in

cutaneous melanoma relative to other cancers [8]. Melanomas harbor a high mutational load (>10 mutations per megabase), included within are a high number of ultraviolet-signature mutations, as discovered through cross-cancer genetic-landscape analysis [9, 10]. Concentrated melanocytes can form melanocytic nevi, commonly called moles. Nevi with abnormal borders, coloring, changes in size, or increases in the number of are a potent risk factor and used as a diagnostic feature [11]. It has been demonstrated that about 81% of patients had a nevus that exhibited some form of change in the location of a malignant melanoma lesion [12]. Mechanisms linking nevi changes to tumorigenesis are still not understood. Common mutations see in melanoma are BRAF, NRAS, PTEN, and p53 mutations. These mutations lead to uncontrolled proliferation, increased aggressiveness, and increased resistance to therapy through increased DNA repair and inhibition of apoptotic pathways. BRAF mutations are the most common mutation seen in melanomas, with 40-60% of melanomas exhibiting a BRAF mutation with the most common being $BRAF^{V600E}$. Interestingly, this mutation is also seen in about 70% of benign nevi, possibly indicating that BRAF mutations do not play prominent roles in the genesis of a melanoma tumor [13].

1.3 Current Melanoma Treatments

While melanoma caught early is highly treatable, advanced stages reduce survivability drastically. Immediate migration to other cutaneous sites or to subcutaneous tissues dramatically drops the response rate to therapies as low as 20%. Melanoma transitioning from the radial to vertical growth phase causes growth into subcutaneous tissues directly from the primary tumor and is associated with chemoresistance [11]. When defining melanoma by the spread of the malignant cells we see that localized melanoma confined to the primary site makes up 83% of cases, while regional spread to lymph nodes and other areas of the skin makes up 9%. Distant metastasized and unknown stages of melanoma make up 4% of cases each. The 5-year survival

rates for melanoma based on these classifications are 99%, 66.2%, 27.3%, and 87.2%, respectively [3].

1.3.1 Radiation

Radiation therapy is sometimes used as an adjuvant therapy to surgery for cutaneous melanoma, yet its role remains controversial due to lack of overall survival benefit. This is often only done for patients with a high risk of recurrence based on characteristics of the melanoma and any past recurrences [14, 15]. Following a lymphadenectomy in node-positive lemaona patients, adjuvant radiation therapy prevents local and regional occurance. With advancements in radiation therapy local containment of melanomas can be achieved using stereotactic radiosurgery and stereotactic body radiotherapy. These technologies can be utilized as a management resource for melanomas that have metastasized to the brain, lung, or liver. Investigation into combinational therapies utilizing targeted therapies and immunotherapies along with radiotherapy are ongoing [16].

1.3.2 Surgical

Surgical resection is the mainstay for non-metastasized cutaneous melanoma. Surgical success in complete removal of melanoma cells is based on accurate diagnosis, stage of disease, removal of a sufficient margin around the tumor, and thickness and depth of primary tumor. When performed properly surgery of primary cutaneous melanoma has a 5 year survival rate of about 92%, but studies have about a 40% recurrence rate for cutaneous melanoma with initial recurrence at the site of the primary tumor or distant skin occurring within 8 month, meaning multiple surgeries are likely to be needed [17, 18]. To prevent local recurrence wide local excision is the current standard of care for localized cutaneous melanoma excision. A wide excision typically extends down to the underlying muscular fascia in order to recover any

vertical growth melanoma cells. Peripheral margins used depend on the type of melanoma, location, and size of the primary tumor. In cases of melanomas on the face a margin larger than 0.5cm is required to ensure complete excision, often resulting in needed reconstruction. For tumors larger than 4mm margins of at least 2cm are required. Melanomas of the head and neck most often affect elderly patients who may not be candidates for surgery. Surgery on the face is often followed with reconstructive surgery to maintain aesthetics. In transit metastatic melanoma is any skin or subcutaneous metastasis greater than 2cm from the primary tumor and satellite metastases are lesions occurring within 2 cm of the primary tumor. Surgery for these lesions is used when feasible, but it is not always the best option and overall response rates drop to about 62% [18, 19].

1.3.3 **Chemotherapy**

Regional chemotherapy treatments as adjuvants or neo-adjuvant therapies are used. Isolated limb perfusion (ILP) and isolated limb infusion (ILI) were developed for as treatments for unresectable melanomas [18, 20, 21]. There is some evidence, but not conclusive, that the response rate was higher in the use of ILP than ILI, but ILP has been seen to result in grade 5 toxicity [18, 22].

Dacarbazine is considered the gold standard for melanoma chemotherapy treatment and is the only monochemotherapy approved by the FDA for melanoma treatment, yet it only has a response rate of about 15-22%, the majority only being partial responses (11.2%) [11, 23]. Dacarbazine has no effect on survival rate with the 5 year survival rate being as low as 2% for some patients [23]. Research into combinatory therapies using Dacarbazine and agents like Cisplatin have reported response rates up to 40% in phase II trials. The “Dartmouth regimen” which is a combination of 4 drugs including Dacarbazine has shown a 55% response rate with

continues maintenance up to 82 months [24]. These treatments combining multiple drugs do often times have the drawback of increasing toxicity [25]. Temozolomide (TMZ) acts as an alkylating agent prodrug and is an analog to Dacarbazine. TMZ also is not photodegradable like Dacarbazine, which is thought to contribute greatly to Dacarbazine's toxicity. Rather than enzymatic degradation like Dacarbazine, TMZ spontaneously degrades at physiological pH into the same bioactive form, a methyldiazonium cation. Methyldiazonium then methylates guanin r ich regions of DNA, primarily N7 and O6 guanine positions, where a carcinogenic lesion then develops [26]. N7 regions are methylated at a greater amount than O6 regions, but O6 regions are much more toxic due to enhanced reparation of N7 regions [27]. Currently, TMZ regimens are utilized to treat metastatic melanoma classified as Stage IV melanoma and is delivered orally as a combinatory chemotherapy due to its excellent bioavailability through the gut. TMZ has been shown to promote tumor shrinkage [28]. The consensus is that the response rate and overall survival between TMZ and Dacarbazine are not significantly different, except for a few outliers [29], but the bioavailability, ability to pass through the blood brain barrier, use as outpatient treatment, and preferential side effects influence physicians to administer TMZ over Dacarbazine in certain situations [30]. Also,

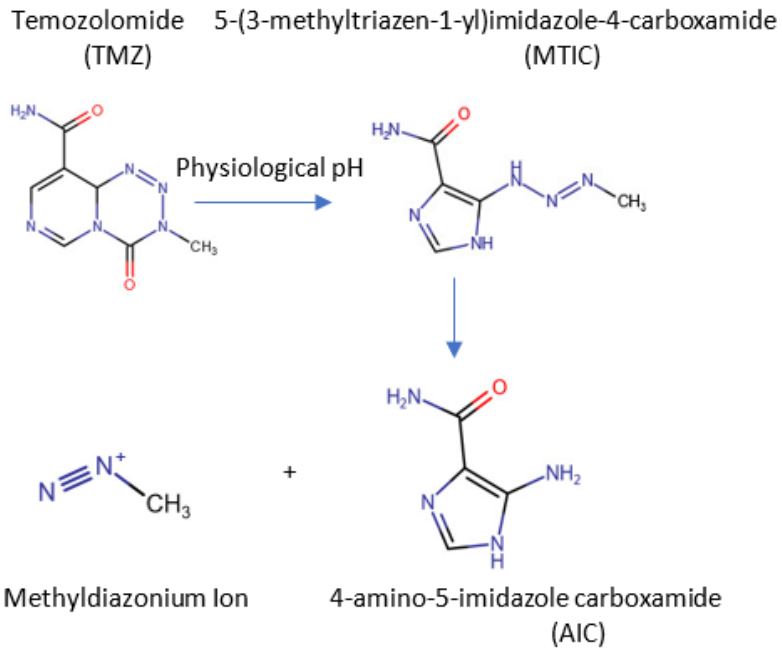

Figure 1: Degradation byproducts of Temozolomide.

patients have reported greater physical functioning in terms of fatigue and insomnia when administered TMZ compared to Dacarbazine [31].

Alternative therapies to surgery for in situ melanoma are currently being researched. The therapy most looked at is an Imiquimod cream that has shown promise for in situ melanoma treatment [32]. Positive results have been shown with significant remission seen and low rates of recurrence [33]. Mechanisms of treatment is thought to be immunological. Imiquimod seems to provoke the immune system into releasing interferon α, IL12, and TNF-α. Melanoma-specific cytotoxic T-cells were present in cutaneous melanoma after Imiquimod treatment [32]. Unfortunately, extreme care must be taken when administering Imiquimod cream due to reports of malignant melanomas arising de novo at the site of application. The cause of these newly formed melanomas is not known so whether this is present in only specific populations is still to be found [34]. Further long-term exposure can lead to immune system toxic effects mimicking traditional immune suppression. Other severe side effects seen include severe muscle weakness, to the point of an inability to walk. In a study using 5% Imiquimod cream on basal cell carcinoma daily for three days the subject fell twice due to weakness, had to be admitted to the emergency room, and administered 125mg of methylprednisolone [35].

1.3.4 **Targeted Therapy**

Melanoma therapies took a turn for the better with the identification of specific BRAF and MEK inhibitors. Vemurafenib and dabrafenib is the most well-known type 1 BRAF inhibitors and most widely used. Initial response to these therapies is generally positive, but progression free survival (PFS) is 6-7 months. Combination of BRAF and MEK inhibitors, such as cobimetinib or trametinib, results in increased PFS when compared to BRAF inhibitors alone [36, 37]. While BRAF is the most common mutation seen in melanomas, they are typically

mutually exclusive with other MAPK protein mutations and there are still significant instances of melanomas not expressing BRAF mutations making BRAF inhibitors meaningless [38, 39]. Further, BRAF and MEK inhibitor acquired resistance remain an active research subject [40].

1.4 Melanoma Chemoresistance

Melanoma exhibits extreme inherent and acquired resistance to chemotherapy agents. This is seen in practice by the abysmal response and survival rate at advanced stages of disease after undergoing chemotherapy treatment. There are numerous known and potentially even more unknown mechanisms behind this resistance, ranging from the ability to efflux drugs, inactive drugs, highly efficient DNA damage repair, and increased anti-apoptotic ability. Initial responses to chemotherapies are often time due to the heterogeneity seen in melanoma tumors, a cell heterogeneity that is higher than other cancers [41]. Melanoma tumors are comprised of several subpopulations, with resistance to chemotherapy agents ranging from low to high [42]. The problem of resistance is compounded when the non-resistance cells are killed off, leaving more room and less competition for the resistance cells, resulting in an increase in aggression and metastasis [43].

Several proteins and pathways have been directly associated with melanoma resistance to alkylating agents. These proteins deal with DNA demethylation, DNA mutation correction, and apoptosis inhibition. Major proteins of interest are microphthalmia-associated transcription factor (MITF), p38 MAPK, TP53, and O-6-methylguanine-DNA methyltransferase (MGMT). Alkylating agents such as Dacarbazine and Temozolomide induce cell cycle arrest by inducing O6-chloroethylguanine DNA lesions via methylation at the O6-position of guanine resulting in O6-methylguanine. O6-alkyguanine DNA alkyl transferase is a DNA repair enzyme that assists

in the repairing of these DNA adducts, reducing melanoma cell death. Melanoma cells exhibit an increase in the repair mechanisms base excision [42, 44]. MGMT is the most studied mechanism of alkylating agent resistance and increase of MGMT activity by 300-fold has been seen in glioblastoma in response to TMZ activity and a strong positive correlation was established between MGMT activity and TMZ resistance [45]. MGMT is expressed in almost all tissues and has been a conserved DNA repair protein vital for DNA integrity and stability [46]. Rather than activating a pathway MGMT acts alone as a suicide enzyme to repair methylated DNA regions. MGMT rapidly recovered in 24-48 hours in trials where researchers attempted to deplete MGMT levels to increase alkylating agent effectiveness. Low-dose, extended-schedule administration of oral TMZ promoted a more sustained MGMT inhibition, but required a higher delivered dose over 5 days than a typical TMZ regimen. MGMT contribution to resistance to melanoma seems to be more dependent on the ability to recognize persistent O6-MeG through other pathways [44].

Glutathione (GSH) levels in many cancer cells are upregulated by as much as 1000 times that of normal cells [47]. This high level of antioxidant is required to prevent the high basal level of reactive oxygen species (ROS) from reaching a lethal threshold. GSH depletion or a reduction in the GSH/glutathione disulfide (GSSG) ratio has been shown to lead to increased sensitivity to several chemotherapy agents. Increased expression of GSH is associated with drug resistance by binding and deactivating chemotherapy agents, reduction of lethal ROS accumulation, preventing DNA and protein damage, or through participating in the DNA damage response.

1.5 Hydrogel-Based Therapies

Injectable hydrogels are utilized to overcome the serious side effects and high dosages seen with systemic drug delivery, as well as decreasing invasiveness of delivery. Injectable hydrogels allow for localized drug release at within the tumor removing the need for excess drug used to

compensate for off-targeting and degradation. Various types of specialized hydrogels have been researched that release their payload in specific scenarios. These include pH-sensitive, photosensitive, and thermosensitive hydrogels. Numerous biocompatible materials are available for hydrogel development [48]. Topical hydrogels have been researched for use in combination with drug injection, and potentially as a standalone treatment. One study utilized an oligopeptide hydrogel loaded with paclitaxel loaded transferosomes. The hydrogel was then spread across the top of the tumor and tumor growth was effectively slowed when used alongside systemic chemotherapy of paclitaxel compared to systemic injection of paclitaxel alone [49].

1.6 Overview of Research Project

This research project focuses on usage of a hydrogel vehicle modified for a specific drug to localize delivery as a means of improving upon conventional systemic chemotherapies. Duke Melanoma 6 cells (DM6), a known highly malignant and chemoresistance strain, and human dermal fibroblast (HDF-α) cells are utilized for all cell studies. DM6 cells are an established model for immunotherapy and chemoresistance, as they are a highly malignant and resistance melanoma cell line. They harbor the melanoma driver mutation $BRAF^{v600e}$ and express the melanoma markers gp100 and MelanA. This cell line is considered to have high clinical relevance as it is extremely resistant to first-line chemotherapy agents and the antigenic expression profile of this cell line has contributed to its utilization as a viable model for evaluating targeted therapies. Human dermal fibroblasts are cells that are responsible for producing the extracellular matrix forming the connective tissue of the skin and play a critical role in wound healing. HDF cells are commonly used in research incorporating skin biology or skin related disorders. HDF are an integral part of the melanoma stroma and constantly interact

with cancers cells. Healthy tissue is important in the healing process after surgical or local chemotherapy usage to treat cutaneous melanoma, and HDF are vital in the role as wound healing cells.

1.7 Goals/Objectives

The goal of this research is to develop a localized method of delivery for TMZ that results in a greater cytotoxicity to highly resistant melanoma cells while also decreasing cytotoxic

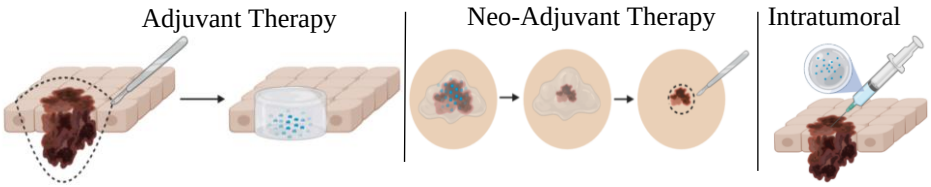

Figure 2: Practical uses of hydrogels as therapies for cutaneous melanomas.

effects to normal cells typically located within the tumor microenvironment. Further, I will explain the mechanism of the cytotoxic effect seen with our hydrogel vehicle that differs from TMZ as a free drug.

1.8 Specific Aims

Aim 1: Determine optimal hydrogel type and TMZ concentration to reduce DM6 cell viability while sustaining HDF-α cell viability and characterize drug release and stability of TMZ loaded CNF and modified CNF.

Local delivery of TMZ in a vehicle capable of retaining the prodrug stability of TMZ could allow for increased effectiveness in primary melanoma cytotoxicity through a slow sustained release rather than a bulk administration. Further, using a bulk administration requires the use of a higher concentration due to the expectation of drug degradation prior to cell interaction and larger drug concentrations are associated with higher off-target cytotoxicity to surrounding normal cells [50]. The focus here is to reach the highest cytotoxicity of DM6 cells with minimal cytotoxicity to HDF-α cells.

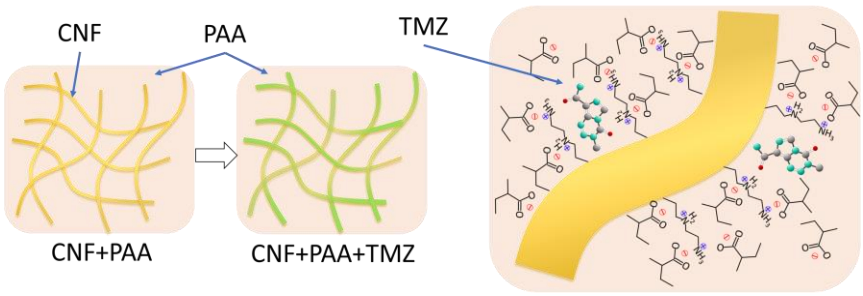

Figure 3: Modification of cellulose to entrap TMZ and create a hydrophobic barrier.

Aim 2: Mimic potential delivery methods of intratumoral injection and topical cream using cells embedded in a 3D collagen matrix and expand number of normal cell lines for safety testing and develop a rational for which physiological pathways to investigate.

Numerous studies have shown significantly different drug concentrations and drug effects between cells seeded on a 2D plane and cells seeded in a 3D matrix [51]. Aim 2 garners more precise information by treating cells seeded in a 3D collagen matrix. Further, the structure of the collagen matrix allows us to mimic intratumoral injection. A consistent and concerning problem with chemotherapy drugs across all cancers, but especially melanoma, is the severe side effects accompanying minimal relief of the cancer cells [52]. The purpose of this aim is to treat both DM6 and HDF-α using an intratumoral injection

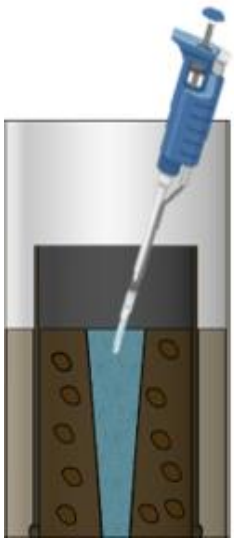

Figure 4: Intratumoral injection into a collagen matrix.

method as the cells are seeded in a more in vivo like environment. In this aim I also plan on introducing cell death inhibitors and activators to develop a hypothesis on the potential causes of increased cytotoxicity when administering our CNF/TMZ treatment.

Aim 3: Determine what methods of chemoresistance are augmented by the localized delivery of TMZ loaded into the hydrogel.

Pointing out the method of chemoresistance that is overcome by using our slow-release method will help in categorizing weaknesses in melanoma that can be taken advantage of. Further, if we can determine targets that are more cytotoxic to melanoma than normal cells when augmented this will provide information on how to effectively treat the disorder while minimizing side effects, which has numerous downstream benefits to the patient. In aim 3 I will focus on assessing oxidative stress agents and antioxidant levels, while also measuring important biomarkers associated with glutathione synthesis, amino acid import, and endogenous cysteine synthesis.

1.9 Innovative Aspects

An innovative aspect of this research is the preparation of a drug delivery vehicle utilizing hydrophobic bonds to protect and deliver a pH sensitive drug that can act as an adjuvant or primary therapy for cutaneous melanoma. As well, this research will demonstrate enhanced cytotoxicity towards a highly resistance melanoma cell line, while exhibiting safer tendencies when compared to a freely given drug.

1.10 Successful Outcome

A successful outcome from this research will provide greater insight into the capabilities of targeted therapies for cutaneous melanomas and demonstrate that increase cancer cytotoxicity

can be achieved while still minimizing loss of normal cells within the tumor microenvironment. Our research will also provide information on how sustained drug delivery, as opposed to traditional bulk delivery, can inhibit various chemoresistant mechanisms associated with malignant melanomas.

Chapter 2: Aim 1: Optimization of TMZ Concentration and PAA Percentage

2.1 Introduction

Injectable hydrogels have garnered much interest and research into their ability to deliver a variety of drug in a minimally invasive way, have a more precise localization of drug delivery, and protect drugs from the external environment allowing for lower dosages and increased bioavailability [53]. Hydrogels offer the ability to deliver a more accurate dosage of drug to required site and minimize off-targeting that could adversely affect healthy tissues. Hydrogels are 3D polymeric networks that can be crosslinked under physical or chemical methods or non-crosslinked, depending on the requirement. They can be hydrated with various liquids allowing for versatility of use with drugs with certain solubility or pH tolerances. By manipulating their material and chemistry hydrogels characteristics such as degradation rate, swelling, and biocompatibility can be fine-tuned [54].

Chemotherapy is still a mainstay cancer treatment, but systemic chemotherapy treatment is baggage with clear undesirable effects. These effects can be severe, such as myelosuppression and neurotoxicity. The inability to specifically target cancer cells and avoid healthy tissue, as well as the large doses required due to limited bioavailability, are two major drawbacks to traditional chemotherapy. Injectable hydrogels offer a solution to these problems. Drugs can now be delivered on site, allowing for a lower dosage, and minimized reaction with healthy tissue [55, 56].

Melanoma chemotherapy is associated with harsh side-effects, so newer methods of delivering drugs that reduce side-effects is needed. Hydrogels have emerged as viable options as dermatological treatments depend on the active compound used and the physiochemical properties of the delivery vehicle. Cutaneous melanoma localized to the skin offers a great opportunity for hydrogels to act a therapeutic delivery systems, whether as injectables, topical creams, or packing gels for post-surgical applications [57]. Pluronic F127 based hydrogels have been used to reduce the increased inflammatory response associated with melanoma tumors and induce apoptosis through the release of ibuprofen. Additionally, this treatment reduced TNF-α-mediated migration in vitro [58].

An important feature of hydrogels is that they can be made using biocompatible materials [59]. Cellulose materials are regarded as excellent candidates for hydrogel synthesis. They are able to hold large amounts of hydrate, highly tunable degradation and mechanical properties, and highly biocompatible. Further cellulose based hydrogels offer the opportunity to be functionalized through their many hydroxyl groups, in order to expand upon their native characteristics [60].

Adjuvant therapy for melanoma patients is recommended based on the risk of cancer recurrence, the stage at which the melanoma was diagnosed, patient age, and comorbidity. Patients with stage III and stage IV melanoma have shown decreased rate of recurrence when surgical resection is followed up with drug-based adjuvant therapy. Toxicity of follow-up therapies is still a hindrance to the wider adoption of adjuvant therapies for lower grade melanomas [61]. Initially ipilimumab, an immune checkpoint blocker, was the first adjuvant therapy to show improvement in recurrence-free and overall survival, but it is associated with high toxicity, so it's relegated to only the most severe cases. Anti-PD-1 agents and BRAF-

targeted therapies currently show more favorable toxicity rates and further increased recurrence-free survival rates, demonstrating that progression in adjuvant therapies is still ongoing [62].

The goal of this aim is to introduce a modified cellulose-based hydrogel intended to provide protection to the pH sensitive drug TMZ, allowing for a sustained release. The cellulose-based hydrogel will act as a hydrophobic barrier to the surrounding medium, thereby maintaining the low-level pH that the hydrogel was originally hydrated with and is conducive to maintaining TMZ in its pro-drug form until eventual release into the more neutral pH medium. Once released the TMZ degrades into its bioactive product. This process is expected to provide a prolonged interaction of drug molecule to melanoma cell compared to bulk delivery of the TMZ as much of the bulk delivered drug will fully degrade into an inactive component before it has a chance to interact with the cells. We also expect normal human dermal fibroblasts (HDF-α) to respond more favorably to a slower release of drug relative to bulk delivery. We will measure cell viability in response to cellulose modified with various percentages of poly-acrylic acid modification, as well as multiple drug dosages. This will provide information on the optimal combination of modified hydrogel and drug dosage to continue use. In this aim we will also be investigating the release characteristics of the hydrogel in a neutral pH medium. This is done to ensure that we see a signal from the TMZ over a prolonged time relative to bulk drug, which is expected to degrade rapidly. We will also investigate the stability of TMZ within the hydrogel when loaded with HEPEs buffer at a pH of 5 without the influence of any surrounding medium in order to evaluate the role the internal environment has on TMZ degradation. The effects of temperature on TMZ stability within the hydrogel will be evaluated to determine the ability to store the drug, as most drugs are typically shipped on ice and expected to retain their cytotoxic properties.

2.2 Experimental Section

2.2.1 Measure cell viability of DM6 cells after administration of various TMZ concentrations within unmodified CNF and four versions of modified CNF

Four versions of modified CNF using PAA at 5, 10, 20, and 30% v/v ratios physically crosslinked were used alongside unmodified CNF and administration of free TMZ. Five concentrations of TMZ were used: 25, 50, 100, 250, and 500uM. TMZ stock was made at 1:1000 ratio using DMSO. The control was DM6 cells in complete (10% FBS) RPMI media without addition of hydrogel or TMZ. Cells were seeded at 2,000 cells/well in 200uL of 10% RPMI media in a tissue-culture treated 96 well plate with a sample size (n) of 4. Cells could adhere for 24 hours prior to administration of treatment. TMZ was initially dissolved in DMSO to make stock solutions of 0.5, 1, 2, 5, and 10mM. These stock solutions were diluted down to working concentrations of 25, 50, 100, 250, and 500uM, respectively. Working concentrations of TMZ were either kept as free TMZ or mixed into the various CNF hydrogels by vortexing for 1 minute and sonicating for 5 minutes to achieve homogenous loading. Free TMZ was administered in 200uL of 10% RPMI media aliquots and hydrogel were added in 30uL aliquots and floated atop 200uL of 10% RPMI media. Cells were incubated at 37˚C for 48 hours at which point the cells were imaged using brightfield microscopy for visual confirmation of cell health. The old media and hydrogel were carefully removed. This was followed by performing an MTS assay with an incubation of 2 hours and measuring absorbance at 490nm using a UV-Vis spectrophotometer. Cell viability for the experimental groups was normalized to the control group and displayed as a percentage.

2.2.2 **Measure potential cytotoxic effects of CNF without drug on DM6 cells**

Potential cytotoxic effects of the hydrogel alone were tested on DM6 cells. Unmodified CNF was compared with 10, 20, and 30% CNF. Unmodified and modified CNF were prepared a explained earlier without the addition of TMZ. Cells were seeded at 2,000 cells/well in a 96 well plate (n=4) with 200uL of 10% RPMI media and left to attach for 24 hours. The control group consisted of cells only and no addition of hydrogel would be added. Hydrogel aliquots of 30uL were then added to the experimental groups. Cells incubated at 37˚C for 48 hours. After 48 hours the hydrogel and old media was removed, and an MTS assay was performed as described earlier.

2.2.3 **Measure HDF-α cell viability with hydrogel and TMZ concentration determined to by most effective against DM6 cells**

Cytotoxicity was also measured against a normal cell population found in proximity to melanoma tumors. CNF and 5% and 10% CNF without addition of TMZ were compared to a control in which no hydrogel was added. The control consisted of cells incubated in 10% RPMI. 2,000 cells/well were added to a 96 well plate (n=4) and allowed to attach for 24 hours. Drug free hydrogel was added to the media in 30uL aliquots, and the cells were incubated for 48 hours. The hydrogel and media were then removed. An MTS assay was performed, and the experimental groups were normalized to the control and displayed as a percentage.

2.2.4 **Measure potential cytotoxic effects of CNF without drug on HDF-α cells**

2mM of TMZ was used as a free drug and loaded into CNF and 10% CNF. A control containing only 10% RPMI media was used. After seeding the cells at a density of 2,000 cells/well in a 96 well plate (n=4) they were incubated at 37˚C for 24 hours. 2mM stock solution

of TMZ was diluted down to 100uM in 10% RPMI media and 200uL was added to the free drug group. The hydrogel types were made and loaded with TMZ, at a working concentration of 100uM, and then 30uL was added to the CNF and 10% CNF groups. Cells were given 48 hours of incubation at 37˚C and the MTS assay was performed after the removal of the hydrogel and old media. Experimental groups were normalized to the control and graphed as a percentage.

2.2.5 Hoechst and Propidium Iodide staining of TMZ and CNF-TMZ treated DM6 and HDF-α cells

Cells were seeded in specially made PDMS devices adhered to glass slides. The PDMS had 8mm holes punched and these served as wells for the cells. Each condition used a separate device containing 4 wells. Cells were seeded at 2,000 cells/well and allowed to attach for 24 hours. TMZ and drug loaded CNF were prepared as explained earlier. Working concentration of TMZ was 100uM and this was given as a free drug, loaded into CNF, and loaded into 10% CNF. Cells were incubated for 48 hours in the presence of the drug at 37˚C. After 48 hours the media was removed and replaced with imaging media containing Hoechst and Propidium Iodide (PI). The staining solution was made by adding 3.3uL of PI and 2.5uL of Hoechst to 10mL of imaging media and warmed up prior to introducing to the cells. Enough staining solution was used to cover the entire bottom of the well and the cells were then incubated at 37˚C for 20 minutes. This is all done while not exposing the cells to a non-sterile environment. Cells were then quickly washed three times in warm 1X PBS and fresh imaging media was then added to the wells. Samples were imaged using a fluorescent microscope and excitation/emission wavelengths of 350/461nm for Hoechst and 594/615nm for PI. All images were taken with a 10X objection and wells were scanned using horizontal passes and 16-20 pictures were taken per well to get the full representation of the cells. 8-bit images were then colored and merged using

ImageJ software. Alive cells from each merged image were counted by discounting cells with red PI stain and that number was calculated towards the total cell count in each merged image. These ratios were then averaged, and the total cell viability was calculated and graphed as a percentage of alive cells to total cells for each respective group.

2.2.6 **Measuring TMZ release from modified and unmodified CNF in a physiological pH buffer**

TMZ was prepared at a 5mM stock solution and loaded into prepared hydrogel forms via sonication to a working concentration of 250uM. 50uL of hydrogel was added to a 1.5mL centrifuge tube and 200uL of 1X PBS pH ~7.4 was added on top (n=4). 10uL of free TMZ was added to 200uL of 1X PBS pH ~7.4 to make a working solution of 250uM, in a 1.5mL centrifuge tube (n=4). Samples were placed in an incubator at 37˚C. At specific time points samples were taken by removing 80uL of supernatant and putting in a UV 96 well plate, along with a 1X PBS blank. 80uL of 1X PBS pH ~7.4 was added back to maintain sink conditions and returned to incubation. Time points taken are (hrs); 0, 1, 2, 3, 4, 24, 48, 72, 96, 120, 144, and 168. Samples were measured at three wavelengths using a UV-Vis spectrophotometer: 266 (AIC), 316 (MTIC), and 325nm (TMZ). Absorbance values were added to an excel sheet and values post-time point 0 were calculated using the dilution factor. Values for TMZ and AIC were plotted as percent change from time 0.

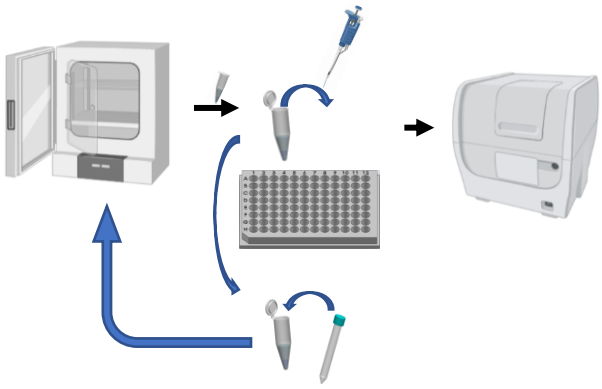

Figure 5: Stepwise method of collection and analysis of TMZ released from hydrogels.

(Absorbance 1 * (80/200)) + Absorbance 2 = Diluted Absorbance Value

Where absorbance 1 equals the previous time point's diluted absorbance value and absorbance 2 equals the absorbance of the time point being calculated.

2.2.7 Measuring TMZ stability within modified and unmodified CNF without outside aqueous influence

Hydrogel samples were prepared with two different hydrating mediums. 1X PBS at a pH of ~7.4 and HEPEs buffer at a pH of ~5 was used to hydrate CNF and 10% CNF samples. TMZ was prepared at a 5mM stock solution and loaded into prepared hydrogel forms via sonication to a working concentration of 250uM. 50uL of hydrogel was added to a 1.5mL centrifuge tube (n=4). Samples were placed in an incubator at 37˚C. Samples were removed at specific time points and 150uL of HEPEs buffer pH ~5 was added on top of the hydrogel. Time points taken were 0, 2, 7, 14, 21, 28, and 35 days. Samples were then vortexed to completely break apart the hydrogel and release its contents into the protective HEPEs buffer. Samples were then centrifuged for two minutes at 5,000g. 80uL samples for measurements were taken from the supernatant and put into a UV 96 well plate. Samples were measured at three wavelengths using a UV-Vis spectrophotometer: 266 (AIC), 316 (MTIC), and 325nm (TMZ). Absorbance values were added to an excel sheet. TMZ results were graphed and normalized to time 0. AIC results were normalized to the samples respective highest peak.

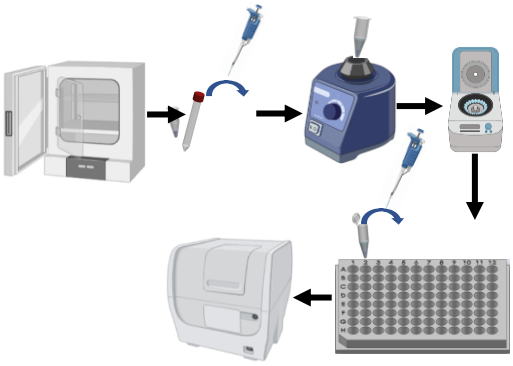

Figure 6: Diagram demonstrating the process of collecting TMZ samples from hydrogels and measuring for a TMZ signal.

2.2.8 **Measuring stability of TMZ at different temperatures**

CNF variants were loaded with 250uM TMZ and hydrated with HEPEs buffer at a pH of 5. When stored at 37C˚ both modified CF variants exhibit the same degradation properties, as well as overall better protection than unmodified CNF. Unmodified CNF showed a sharp decline in TMZ signal between 2 and 7 days, with complete degradation occurring at 14 days, while both modified CNF groups sustained TMZ out to 28 days when incubated at 37C˚. Unmodified CNF and 5% and 10% crosslinked CNF showed a similar pattern to their non-crosslinked variants (Figure 4A). When stored at 4C˚ all groups indicated dramatically prolonged retention of TMZ, with CNF and 10% CNF retaining a greater than 50% signal at 42 days and 5% staying at 35% of time 0. Temperature can affect the pH of a solution so at each time point a sample of the HEPEs buffer kept at 4C˚ used to load the hydrogel was tested for pH change and no change was observed from the original pH value of 5 (data not shown).

2.3 Results and Discussion

2.3.1 DM6 Cell Viability

Initially we found that both group type and concentration had a significant impact on cell viability (P-values; <0.0001 and 0.0178, respectively), so we can say that while both have a significant impact the type of group chosen has the greatest impact on cell viability. A significant difference was found between CNF and 10% CNF at 100uM TMZ, as well as free TMZ and 10% CNF at 100uM TMZ. There was no significant difference found between 10% CNF at the various TMZ concentrations, but the biggest disparity occurred between free TMZ and 10% TMZ at 100uM TMZ, so it was decided to continue with 10% CNF loaded with 100uM TMZ based on these results and the assumption that a lower dosage would be less cytotoxic to

normal cells. After determining that 10% CNF loaded with 100uM TMZ was likely our optimal combination we wanted to confirm this by measuring cell viability using 5% CNF and 25uM and 50uM TMZ concentrations. No significant difference was found between the 5% CNF and 10% CNF regardless of TMZ concentration, but 100uM free TMZ was significantly different from both 5% CNF and 10% CNF at 100uM and had the largest disparity among the concentrations. Based on a repeated study that continued to show 10% with a lower, but not quite significant difference we decided 10% CNF would be our optimal combination from here on. Since the hydrogel will be in direct contact with cells, we needed to determine whether the decrease in cell viability we were seeing was from the TMZ or from the modifications applied to the CNF. Our results showed no significant different between control (media only) and CNF or any version of modified CNF in terms of cell viability.

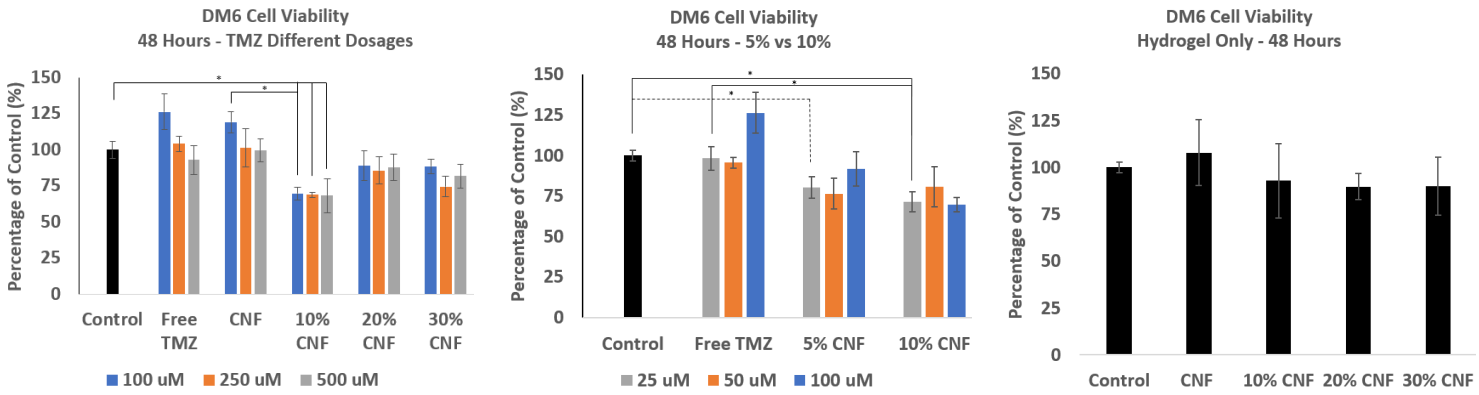

*Figure 7**: Measuring cell viability of different modified CNF and different TMZ concentrations:** (A) MTS cell viability assays were performed after treating DM6 melanoma cells seeded in 96 well plates with the corresponding concentrations and modified CNF hydrogels for 48 hours. (B) 100uM loaded into 10% CNF was determined to be the most effective, so for further optimization cell viability was measure using concentrations of 25uM, 50uM, and 100uM, and including 5% modified CNF alongside 10% CNF. Ultimately 100uM loaded into 10% CNF was decided as the optimal treatment. (C) To ensure it was the drug interaction promoting the cytotoxicity and not the hydrogel itself, the CNF without TMZ loaded was incubated for 48 hours and using MTS was found to not have significant cytotoxicity effects.*

2.3.2 HDF-α Cell Viability

We found that neither CNF nor any version of modified CNF that we measured had any significant effect on cell viability. When adding 100uM of TMZ to the hydrogel we see at that

concentration there was no significant effect on HDF-a cell viability between 10% CNF and the control. 10% CNF DM6 cell viability showed a significant difference in the decrease of cell viability relative to both control and free TMZ, as well as a significant difference in cell viability with 10% CNF HDF-a, with the HDF-a cells having a higher cell viability. The result from the 10% CNF showed that we were able to reverse the effects seen by the free TMZ and provide a killing effect to the DM6 melanoma while not having any significant effect on the HDF-a by using the 10% CNF.

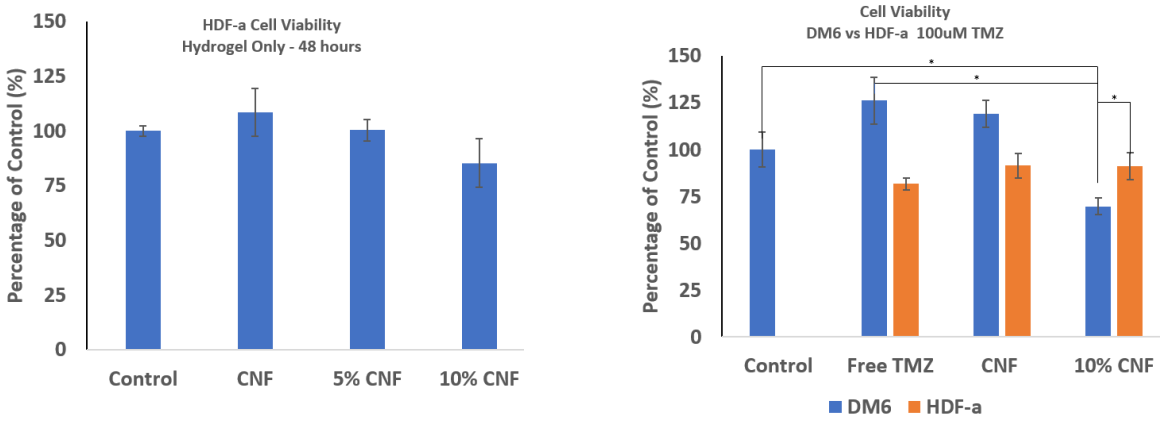

Figure 8: ***Cell Viability of Normal Human Dermal Fibroblast-adult Cells:*** *(A) To confirm the potential for off-target cytotoxicity HDF-a cells were incubated with CNF, 5% CNF, and 10% CNF without the drug and an MTS assay was performed to measure cell viability. (B) After confirming the hydrogel alone had to cytotoxic effects, TMZ at a concentration of 100uM was loaded into unmodified CNF and 10% CNF, as well as delivered as a free drug. MTS assay was performed on both studies to quantify cell viability. Cell viability was then normalized to the control group.*

2.3.3 **Hoechst and PI Staining:**

We found greater disparities between the free TMZ group and 10% CNF group with both cell lines compared to MTS assay. One potential reason for this is that treated cells could have expressed increased levels of glutathione, associated with oxidative stress, which can interfere with MTS assay and cause a higher absorbance level. Significant differences were found between HDF-a control and HDF-a treated with free TMZ, demonstrating a severe cytotoxic effect on HDF-a when TMZ is administered as a free drug. No significant difference was found

between HDF-a control and HDF-a treated with 10% CNF loaded with TMZ. 10% CNF loaded with TMZ had a significantly less cytotoxic effect on HDF-a compared to the free drug treatment, indicating a safer method of delivery using the same drug. Our DM6 results were quite different and highly desirable. We found a high significant difference between DM6 control group and DM6 treated with 10% CNF loaded with TMZ and a significant difference between DM6 treated with free TMZ and DM6 treated with 10% CNF loaded with TMZ. These results demonstrate a promising method of TMZ delivery that is both highly cytotoxic to DM6 cells and much safer for HDF-a cells compared to administration of TMZ as a free drug.

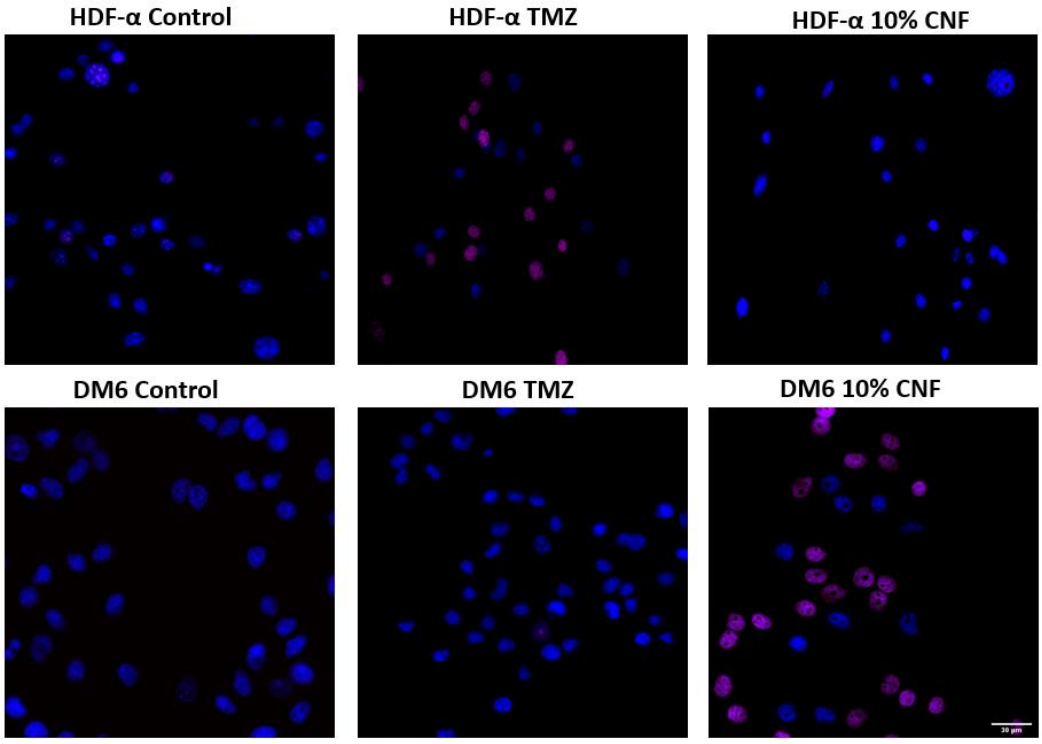

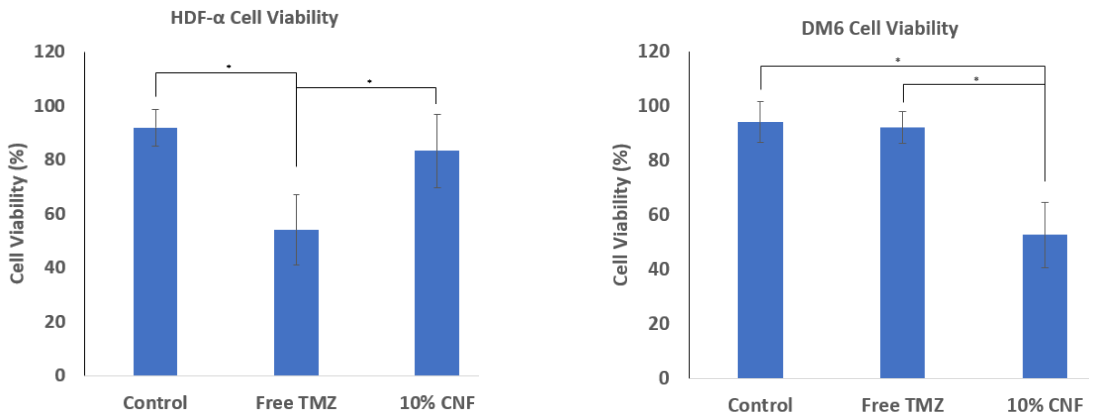

Figure 9: ***Live/Dead cell staining on DM6 and HDF-α cells:*** *Live/Dead cells staining was performed on DM6 and HDF-α cells after treatment with 100uM TMZ administered as either a free drug or loaded into a 10% CNF hydrogel. Cells had been seeded in a specially made PDMS device attached to a glass slide and incubated for 48 hours and were imaged at excitation/emission wavelengths of 350/461nm for Hoechst and 594/615nm for PI using a 10X objective.*

2.3.4 **Wet Release Study**

Drug release studies demonstrated that by loading TMZ into a hydrogel vehicle we were able to maintain a signal longer than Free TMZ. Unmodified CNF and 10% CNF/TMZ displayed a signal for TMZ out to 72 hours, while AIC remained for 168 hours. The signal for Free TMZ diminished rapidly and was gone by within 24 hours. The trend of release for both CNF and 10% CNF were similar indicating that the addition of PAA does not influence the release profile of TMZ.

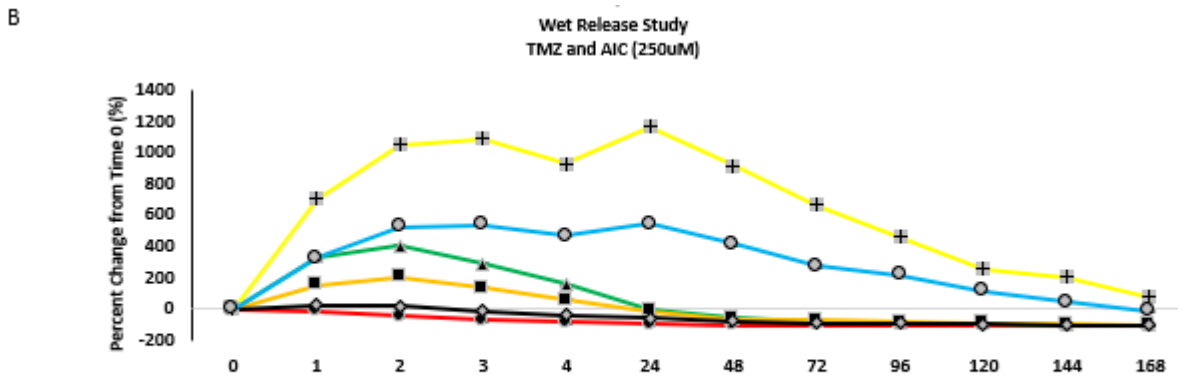

Figure 10: ***Collection of released TMZ from hydrogel into external medium:*** *(A) 250uM concentration of TMZ was either loaded as free TMZ into 1.5ml centrifuge tubes or into unmodified or 10% CNF (hydrated with HEPEs buffer pH 5) with 700uL of PBS pH 7.4 loaded on top and placed into an incubator at 37˚C. Immediate time points from 0-4 hours were taken as the half-life of TMZ in neutral pH is about 1.8 - 2.5 hours. Time points were taken every 24 hours, from time 0, after that. Measurements were done at 325nm (TMZ) and 266nm (AIC). 80uL of fresh 1X PBS was added back into the centrifuge tube to retain sink volume and then placed back into the incubator. (B) TMZ signal was retained over a longer period when loaded into either CNF or 10% CNF compared to free TMZ. This is also indicated by the continuous signal obtain by the TMZ byproduct AIC. Signals above 0 indicate that release is occurring, while anything below 0 indicates that release has stopped, and any product left in the medium is now only degrading. A positive slope indicated a release rate that is higher than the degradation rate, while a negative slope indicated a degradation rate that outpaces the release rate.*

2.3.5 **TMZ Stability Study**

Either CNF or 10% CNF when hydrated with HEPEs buffer pH ~5 was able to retain a TMZ signal over twice as long as the hydrogel when hydrated with 1X PBS pH ~7.4. We found that 10% CNF retained TMZ it its prodrug form four weeks longer than CNF when both were hydrated with HEPEs Buffer pH ~5.

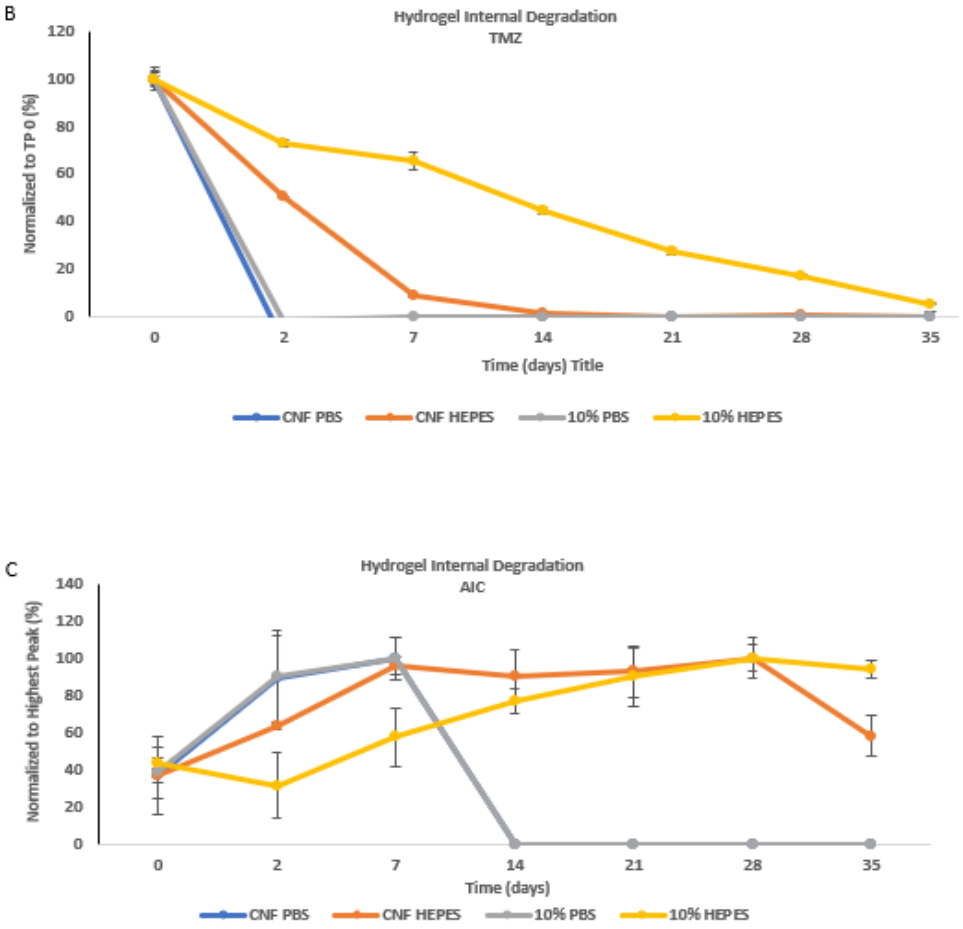

Figure 11: ***Collection of TMZ from hydrogel matrix:*** *(A) Samples were collected from incubation at designated time points and 150uL of HEPEs buffer pH 5 was added over the hydrogel. Tubes were then vortexed to cause maximum release of TMZ, and then spun down to avoid gel contaminations. 80uL of sample was taken and measured in a UV-vis plate at 325nm (TMZ) and 266nm (AIC). (B) TMZ signal, measured at 325nm, was taken after the hydrogel was broken down to allow separating out of the remaining TMZ. No sample was used for more than 1 time point and TMZ degradation was able to be measured out to 35 days for 10% CNF indicating an ability to retain the original pH of the hydrate which allowed for better TMZ stability compared to all other groups. Hydrogels hydrated with 1X PBS pH 7.4 had immediate TMZ degradation, as expected. (C) AIC, measured at 266nm, represents the byproduct of TMZ and has a longer half-life, so indication of a plateau of AIC signal shows a steady more prolonged stability of TMZ that would allow for a maintained supply of AIC. 10% CNF maintains a higher AIC value out to 35 days corroborating the data from figure 4B that 10% CNF maintains a better environment for TMZ stability over a longer time compared to all other groups.*

2.3.6 **Effect of temperature on TMZ stability**

When stored at 37C˚ both modified CF variants exhibit the same degradation properties, as well as overall better protection than unmodified CNF. Unmodified CNF showed a sharp decline in TMZ signal between 2 and 7 days, with complete degradation occurring at 14 days, while both modified CNF groups sustained TMZ out to 28 days when incubated at 37C˚. When stored at

4C˚ all groups indicated dramatically prolonged retention of TMZ, with CNF and 10% CNF retaining a greater than 50% signal at 42 days and 5% staying at 35% of time 0. Temperature can affect the pH of a solution so at each time point a sample of the HEPEs buffer kept at 4C˚ used to load the hydrogel was tested for pH change and no change was observed from the original pH value of 5 (data not shown).

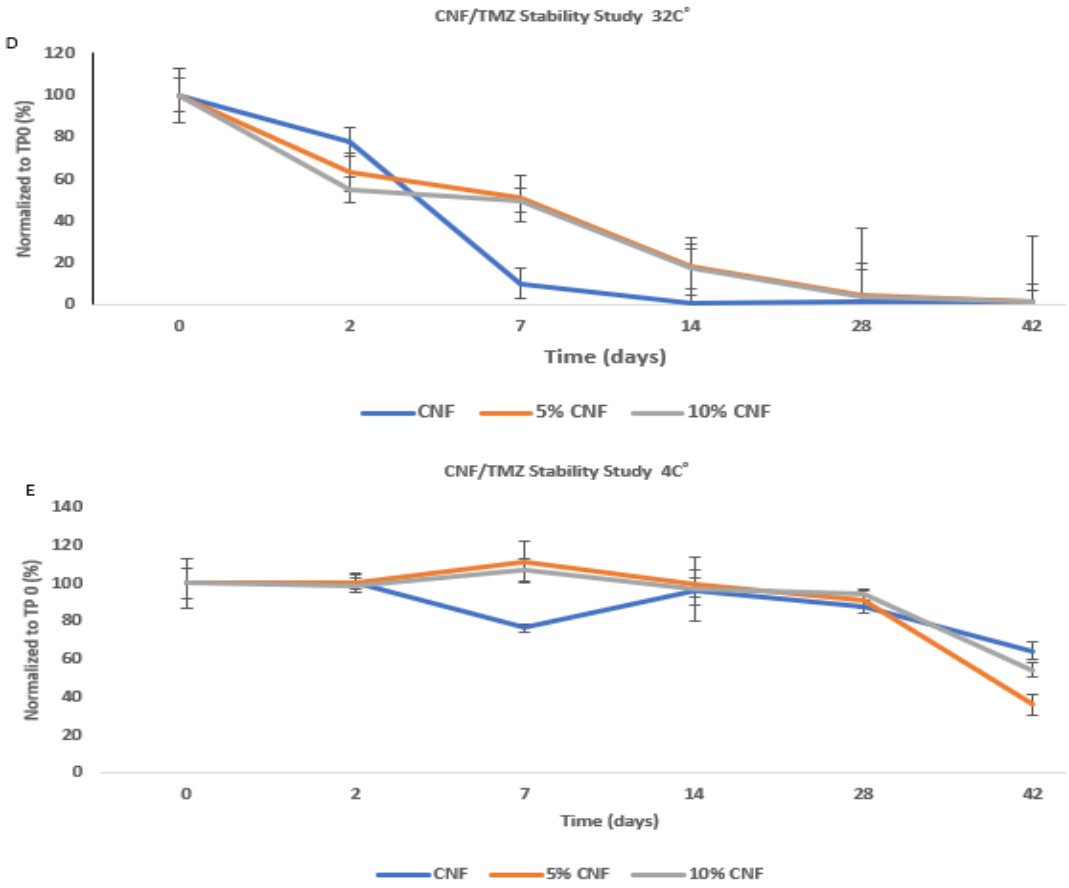

Figure 12: ***TMZ Stability in CNF Hydrated with HEPEs Buffer pH 5 at Different Temperatures****: (D) TMZ retention was improved by modification of CNF, also seen in Figure 4A, over unmodified CNF. 5% and 10% modified CNF versions sustained a TMZ signal twice as long as unmodified CNF, 28 and 14 days respectively when stored at 32°C. (E) Temperature plays a large role in the ability of our hydrogel to preserve TMZ, regardless of the addition of PAA or not. All CNF variants continued to show substantial TMZ signal out to 42 days, unmodified and 10% CNF remaining above 50% and 5% CNF above 35% from time 0 at 4°C.*

2.4 Summary

Cell viability assay confirmed that all versions of the hydrogel were biocompatible regardless of cell type. DM6 showed high resistance to free TMZ at all concentrations studied, but especially high viability at 100uM. A possible explanation is that 100uM was strong enough to elicit a metabolic response, but not enough to cause any harm. A metabolic response would include the expression of reduced glutathione, which cells express in times of stress related to DNA damage, but reduced glutathione can also non-enzymatically degrade the MTS agent tetrazolium ultimately causing a higher absorbance related more to the increased metabolic activity than actual cell viability. DM6 cells showed a significantly reduced cell viability when TMZ was loaded into the 10% CNF, regardless of concentration. The lack of cell viability change with drug concentration change is possibly due to there being subpopulations of DM6 cells and none of the concentrations were potent enough to affect the highly resistant cells, but all concentrations could kill off the less resistance cells. Our results showed that TMZ loaded into the 10% hydrogel was significantly less cytotoxic to HDF-α cells than DM6 cells. While there was no difference in the trend of TMZ release between CNF and 10% CNF, both hydrogels retained a TMZ signal over 24 hours longer than free TMZ. 10% CNF did show a substantially longer period of TMZ stability compared to CNF when both hydrogels were hydrated with HEPEs buffer pH ~5. Our stability study with a temperature difference shows that

Chapter 3: Aim 2: Cytotoxicity Testing in a 3D Collagen Matrix

3.1 Introduction

2D in vitro cell cultures are limited in their relevance to in vivo effects as cellular physiology and response is highly mediated by their 3D extracellular environment they would experience within the body. Cell culture systems designed to provide a bridge between 2D, and in vivo environment are becoming more popular as data becomes available demonstrating their reliability in predicting future in vivo response. These 3D environments vary in their design and complexity. Data has shown that cells cultured in a 3D environment differ from their 2D counterparts in morphology and protein/DNA expression profiles resulting in varying degrees of growth, proliferation, and drug sensitivity [63, 64]. There is a large diversity of materials used to create 3D culture systems for cancer research, some commonly utilized materials include basement membrane extracts from tumors, hyaluronic acid, and collagen type I. Collagen type I makes up the largest proportion of collagen in the skin, especially in younger people, and so can be utilized for the creation of a 3D matrix for melanoma cell culturing [65].

Ferroptosis is a newer studied mechanism of cell death that relies on oversaturation of iron content leading to oxidative stress and cell membrane leakage. This cell death type is considered because cancer cells typically have higher basal levels of iron and ROS production due to high metabolic levels relative to normal cells and melanoma cells have been identified to undergo ferroptosis when treated with alkylating agents. It is thought that cancer cells might be more sensitive to this type of cell death [66], which could provide an explanation as to why our treatment invokes a lower cell viability of DM6 compared to HDF-α cells. To assess whether ferroptosis is occurring we will be utilizing two known ferroptosis activators, Erastin and RSL3 and two ferroptosis inhibitors, ferrostatin-1 and deferoxamine (DFO). Erastin is an inhibitor of

the cystine-glutamate antiporter system Xc- (also known as SLC7A11). This prevents cystine uptake decreasing production of cysteine, an amino acid crucial for glutathione synthesis [67]. RSL3 binds and inactivates glutathione peroxidase 4 (GPX4). GPX4 protects cell membranes from lipid peroxidation [68]. Ferrostatin-1 actively reduces accumulation of lipid hydroperoxides [69] and DFO acts as an iron chelator, binding to the increased iron required for ferroptosis [70].

Melanoma cells are known to be apoptotic deficient [71] while normal cells naturally prone to all types of apoptosis for homeostatic reasons. The difference in cell viability between DM6 and HDF-α cells when treated with either free TMZ or CNF/TMZ could possibly be that separate mechanisms of cell death are being activated in response, with a CNF/TMZ promoting a response that cancer cells are more sensitive to and free TMZ a response normal cells are more sensitive to. Z-VAD-FMK is a caspase-dependent apoptosis inhibitor by inhibiting caspase -1 to -10 [72].

Cancer cells can be more sensitive to an increase in ROS production or glutathione (GSH) depletion, resulting in severe oxidative stress that passes the lethality threshold. Oxidative stress can be initiated in numerous ways, but GSH is the primary antioxidant in cells, so GSH supplementation is provided as means to determine whether oxidative stress is a promoter in the cell death being seen [73].

Buthionine sulphoximine (BSO) is an inhibitor of glutathione synthesis and commonly used to deplete GSH levels. BSO specifically inhibits γ-glutamylcysteine synthetase, the enzyme required in the first step of GSH synthesis [74].

The goal of this aim is to introduce our cells into a more in vivo like environment to get a sense of what CNF/TMZ dosage is more applicable to a 3D environment where cancer cells are

likely going to be less sensitive to the drug relative to 2D cultured cells. Our 3D model is made of collagen type I polymerized using heat incubation. Having our cells embedded in this gel allows up to also mimic the delivery that our gel is designed for, this being intratumoral injection. By injecting into the gel, we can get a sense of whether injecting our hydrogel is a viable option for delivery and how well the drug interacts with the cells.

The second goal of this aim is to evaluate candidates of cell death related pathways as to whether they are being utilized by our CNF/TMZ treatment to overcome DM6 chemoresistance. Using a panel of molecules to inhibit or activate certain methods of cell death we can determine which method is more likely. This will determine further evaluations of specific pathways and molecules.

3.2 Experimental Section

3.2.1 **Cell viability of DM6 cells loaded into a 3D collagen matrix treated with unmodified CNF, 10% CNF, and free TMZ**

TMZ stock solutions are prepared at 2, 5, 10, and 20mM concentrations. Hydrogel variations used are CNF and 10% CNF are prepared and loaded with drug at working solutions of 100, 250, 500, and 1000uM TMZ working solutions as mentioned earlier. Type 1 collagen matrix is prepared by adding 0.5mL of collagen into 1mL 10% RPMI media and 12uL 1N sodium hydroxide for pH adjustment. Cells were then seeded at a density of 3,000 cells/well. 250uL of collagen is pipetted inside a cast made from a 0.6mL centrifuge tube. Casts are put in 48 well plates and 300uL of media is added to the outside. Enough media is added to maintain cells, but not cover the top of the collagen matrix. The amount of media to use was determined by calculating the volume of a hollow cylinder using the known volume of the collagen, height of collagen, and area of a single well in a 96 well plate. Cells are given 24 hours to acclimate to

the collagen environment and then TMZ is injected into the center of the collagen matrix or applied on top of the collagen matrix as a free drug or loaded into the CNF and 10% CNF hydrogel. The control group has 10uL of 1X PBS injected. Cells are then incubated for 48 hours at 37˚C. MTS assay is performed by adding 200uL of working MTS solution into the cast and allowed one minute to seep through the collagen matrix. The cast is then removed leaving behind the collagen matrix in the well plate. Cells are then incubated for 2.5 hours. 80uL of sample is transferred to a new 96 well plate which is then read at 490nm using a UV-Vis spectrophotometer. Cell viability for the experimental groups was normalized to the control group and displayed as a percentage.

3.2.2 Cell viability of HDF-a loaded into a 3D collagen matrix treated with unmodified CNF, 10% CNF, and free TMZ

Cells are treated through an injection and topical stye of delivery. TMZ is given at working concentrations of 100, 250, 500, and 1000uM as free drug or loaded into CNF hydrogel or 10% CNF hydrogel. Prior to treatment cells are seeded into 3D collagen matrices at 3,000 cells/well and placed into 48 well plates with 300uL of 10% RPMI media. Cells are assimilated for 24 hours and then treated for 48 hours. A group that was not given any treatment was used as a control. MTS assay is performed after 48 hours by adding 200uL of working MTS solution and incubating for 2.5 hours. 80uL of sample is removed and placed into a 96 well plate for measurement by a UV-VIS spectrophotometer at 490nm and then results are normalized to the control group.

3.2.3 **Cell death analysis using a panel of death activators and inhibitors**

In order to narrow down possible mechanisms of cell death resulting from our treatment DM6 cells were treated with ferroptosis activators and inhibitors, glutathione synthesis inhibitors, glutathione supplementation, and a caspase-dependent apoptosis inhibitor. BSO was added 16 hours prior to the addition of any other treatments. Provided in the table below are the treatments used for DM6 and HDF-α. After 48 hours of treatment the media solution was removed, and MTS assay was performed.

Table 1: ***AIM 2 treatments used in cell studies.***

DM6	HDF-α
Control	Control
Free TMZ (250uM)	Free TMZ (250uM)
Free TMZ + BSO (250uM, 100uM)	Free TMZ + Z-VAD-FMK (250uM, 10uM)
CNF/TMZ (250uM)	Free TMZ + DFO (250uM, 100uM)
CNF/TMZ + Z-VAD-FMK (250uM, 10uM)	Free TMZ + GSH Suppl (250uM, 5mM)
CNF/TMZ + DFO (250uM, 100uM)	CNF/TMZ (250uM)
CNF/TMZ + GSH Suppl. (250uM, 5mM)	CNF/TMZ + Z-VAD-FMK (250uM, 10uM)
CNF/TMZ + Ferrostatin-1 (250uM,8uM)	CNF/TMZ + DFO (250uM, 100uM)
CNF/TMZ + BSO (250uM, 100uM)	CNF/TMZ + GSH Suppl. (250uM, 5mM)
Erastin (8uM)	CNF/TMZ + BSO (250uM, 100uM)
RSL3 (0.5uM)	
Erastin + GSH Suppl (8uM, 5mM)	
RSL3 + GSH Suppl (0.5uM, 5mM)	

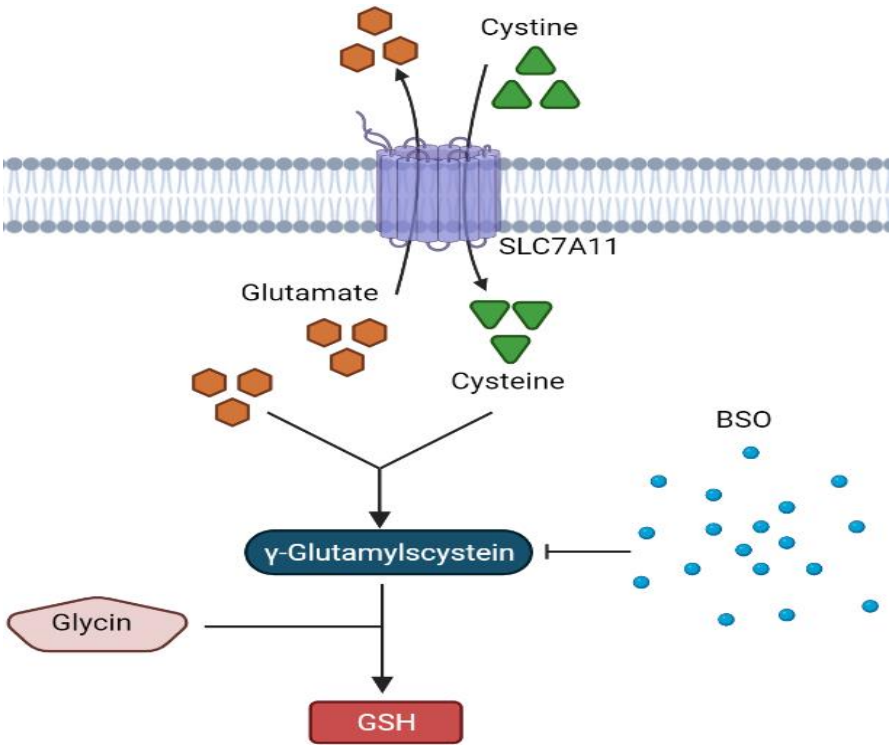

Figure 13: ***Buthionine Sulphoximine (BSO):*** *BSO reduces levels of glutathione by inhibiting γ-glutamylcysteine synthetase, the enzyme required in the first step of glutathione synthesis. This results in inhibition at a more critical point compared to Erastin.*

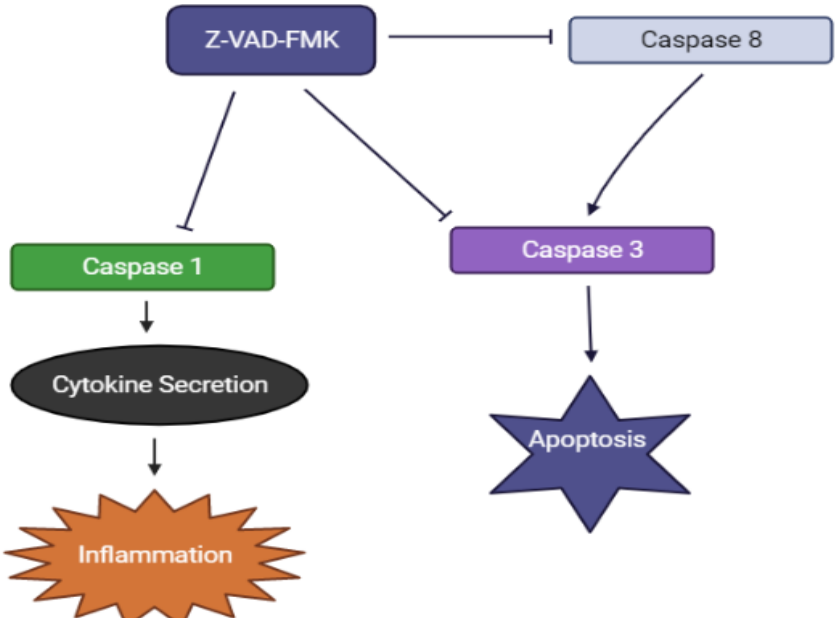

Figure 14: ***Z-VAD-FMK****: Z-VAD is an irreversible pan-caspase inhibitor that binds to the catalytic site of caspase proteases to inhibit apoptosis induction. In some instances, Z-VAD has been seen to induce necroptosis by Caspase 8 inhibition.*

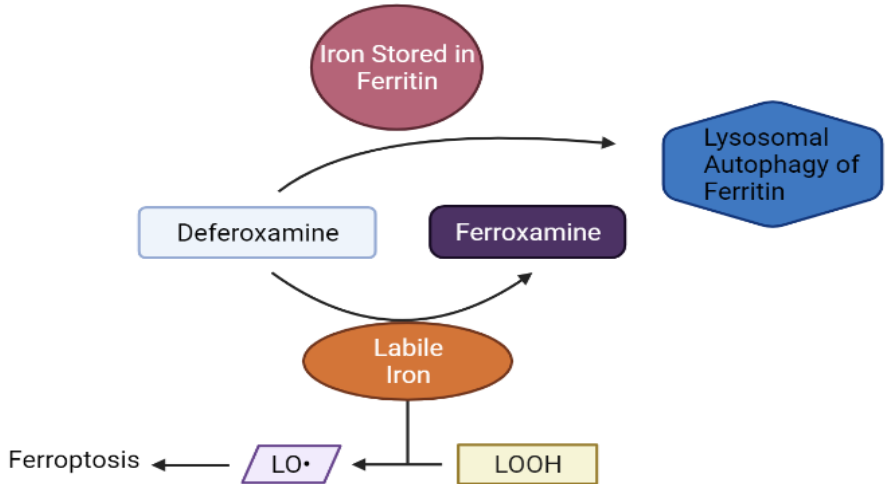

*Figure 15: **Deferoxamine**: Deferoxamine (DFO) is an iron chelator known for its prevention of ferroptosis by decreasing intracellular labile iron levels. DFO binds to labile iron forming the molecule Ferrioxamine which renders the iron unavailable for chemical reactions which prevents formation of lipid radicals (LO·). Further, DFO can induce autophagy in order to degrade ferritin in lysosomes, reducing the ability of the cell to store iron.*

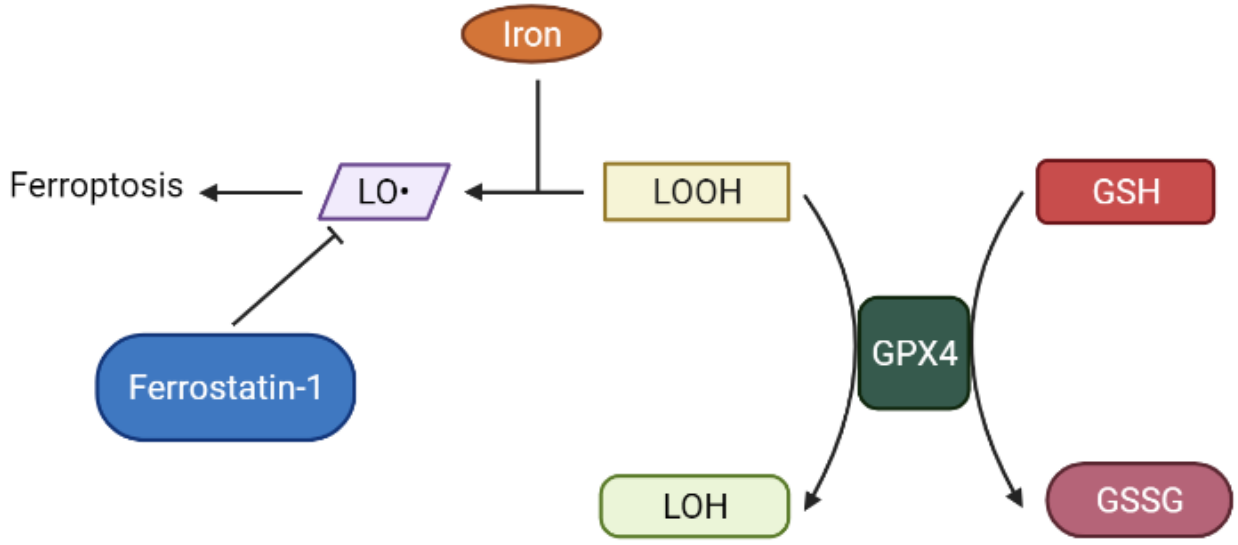

Figure 16: Ferrostatin-1: Ferrostatin-1 prevents ferroptopic cell death by acting as a radical trapping antioxidant and preventing the accumulation of lipid hydroperoxides (LOOH and lipid radicals (LO·). GPx isozymes can catalyze the reduction of LOOH to corresponding alcohols (LOH).

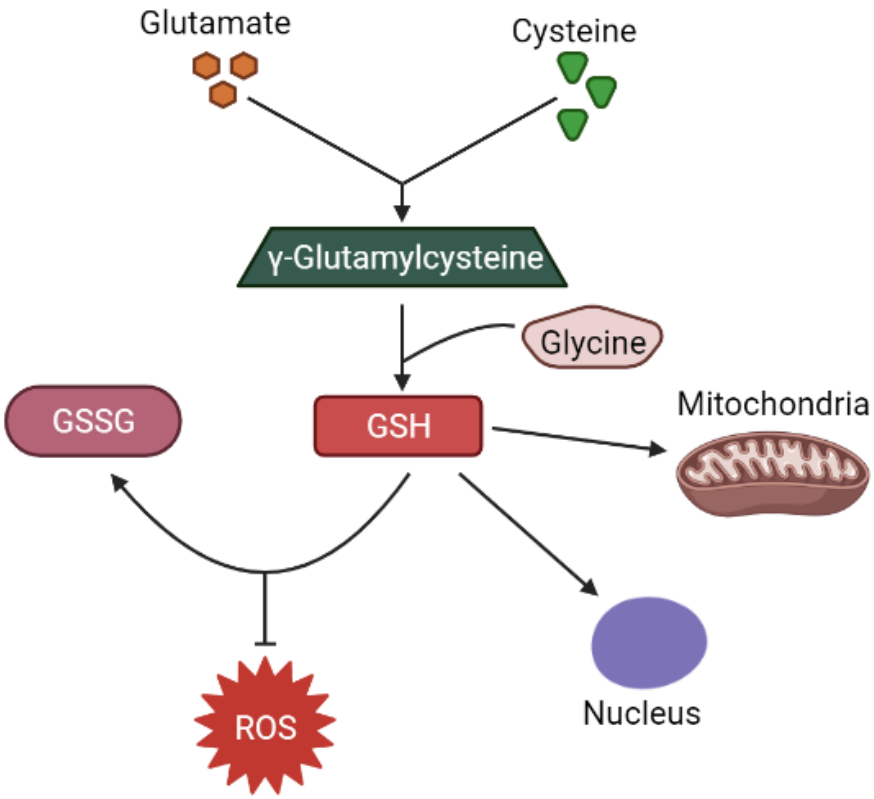

*Figure 17: **Glutathione Synthesis**: The first step in glutathione (GSH) synthesis is the formation of γ-glutamylcysteine through the interaction of glutamate and cysteine. Cysteine is considered the rate-limiting enzyme for GSH synthesis. γ-glutamylcysteine, with glycine, are then able to form GSH. GSH has numerous responsibilities within the cell, the primary being to act as an antioxidant where it is oxidized to glutathione disulfide (GSSG). GSH can also be imported into the mitochondrial and the nucleus of the cell, as well.*

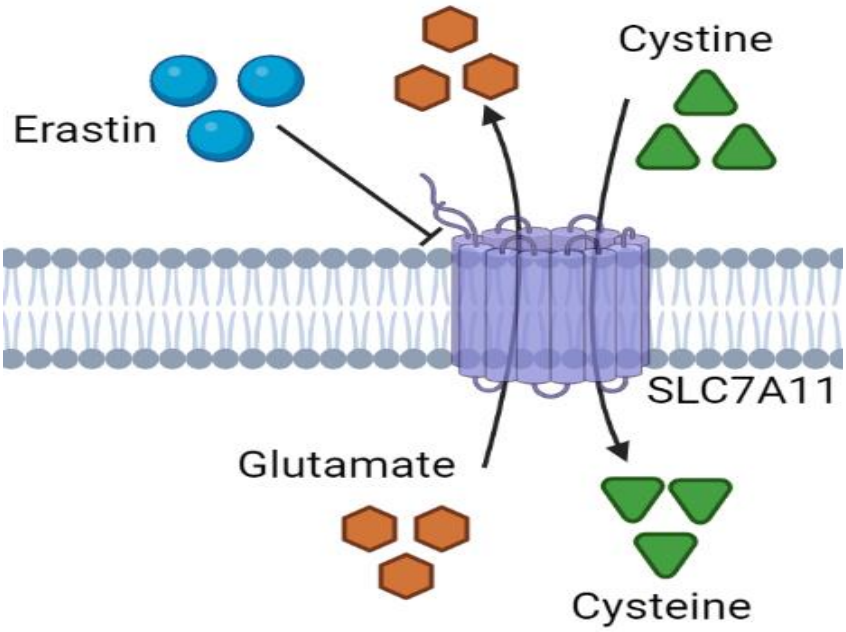

*Figure 18: **Erastin**: Erastin is a small molecule commonly used for the initiation of ferroptosis. Erastin functionally inhibits the cystine/glutamate antiporter SLC7A11 (system XC-). This inhibition can result in an inability to produce efficient glutathione and cystine is reduced into cysteine, the rate-limiting enzyme for glutathione synthesis.*

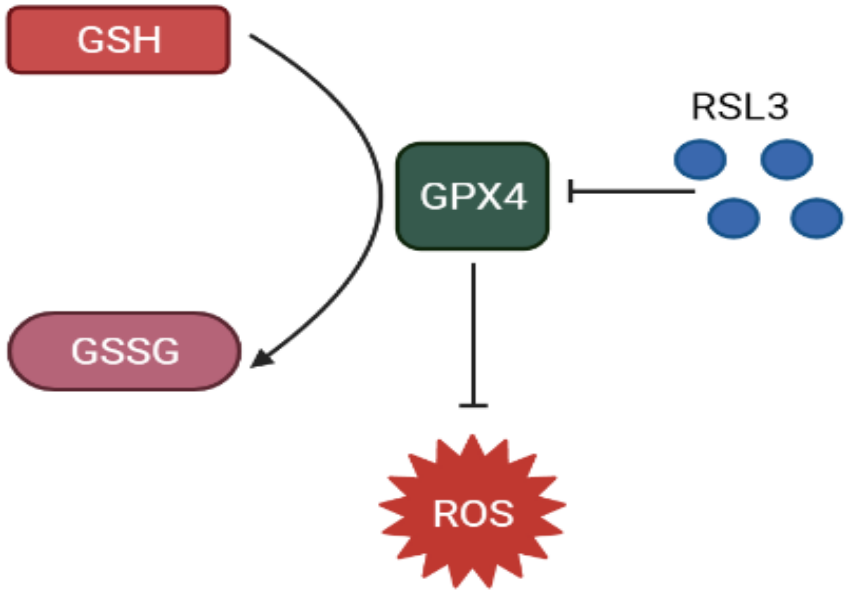

Figure 19: RSL3: Glutathione peroxidase 4 (GPX4) is a phospholipid hydroperoxidase that protects cells against cell membrane peroxidation. GPX4 reduces hydrogen and lipid peroxides by through reduction of glutathione (GSH) into glutathione disulfide (GSSG). RS L3 activates ferroptosis cell death by inhibiting GPX4 activity, causing an accumulation of hydrogen and lipid peroxidation resulting in increased oxidative stress and cell membrane peroxidation.

3.3 Results and Discussion

3.3.4 **DM6 cell viability using injection delivery of TMZ**

Transitioning from 2D cell culturing to a 3D collagen matrix allows for us to mimic an intratumoral delivery, as well assess the ability of TMZ to traverse through a 3D environment. We found that a higher concentration of TMZ was required compared to 2D cell culture, which makes sense because the TMZ now has a much larger area to cover, and it will degrade before it has time to reach any cells. Low amounts of TMZ, whether free or loaded into 10% CNF initiated a high response by the cells, which is likely more a metabolic response than an increase in cell proliferation. At 1000uM we see a significant difference between the free TMZ and 10% CNF, with the 10% CNF attaining an 80% cell viability, while free TMZ remains near 100%. Further we show that 10% CNF without drug does not have any negative effect on cell viability.

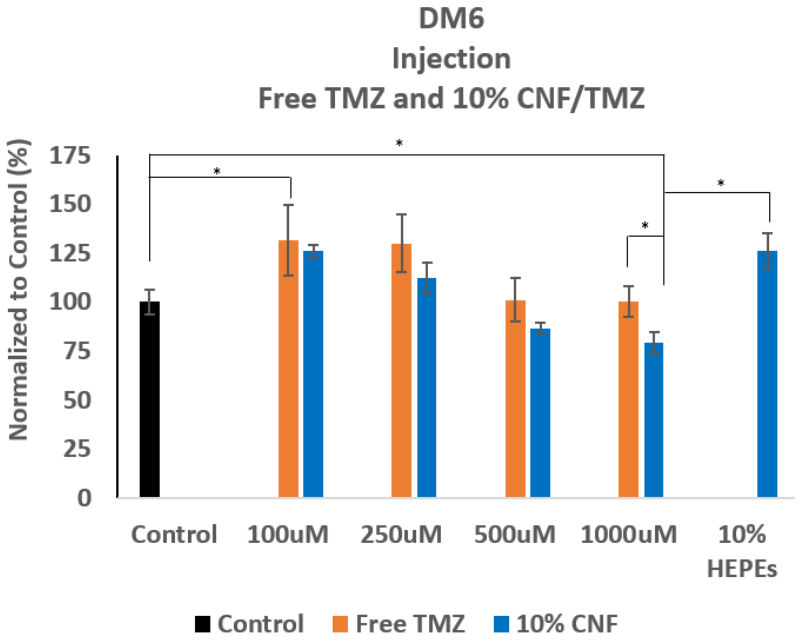

Figure 20: ***DM6 cell viability using injection delivery of hydrogel loaded with TMZ:*** *DM6 cells seeded in a 3D collagen matrix were treated by an injection style delivery of 10% CNF loaded with either 100uM, 250uM, 500uM or 1000uM TMZ. Another group was injected with 10% hydrogel absent of TMZ. Cell viability was measured using an MTS assay and the results were normalized to the control group.*

3.3.5 **HDF-α cell viability using injection delivery of TMZ**

Decreasing off-target cytotoxic effects is of high priority and this study provides important information regarding the increased safety that 10% CNF provides. Significant differences are seen between free TMZ and 10% CNF TMZ with both concentrations. The most dramatic is seen at 1000uM, where HDF-α cell viability falls below 15% when free TMZ is administered but maintains a cell viability above 70% when TMZ is administered loaded in 10% CNF. These results indicate that at 500 uM and 1000uM we can maintain a healthy population of HDF-α cells when treated with 10% CNF.

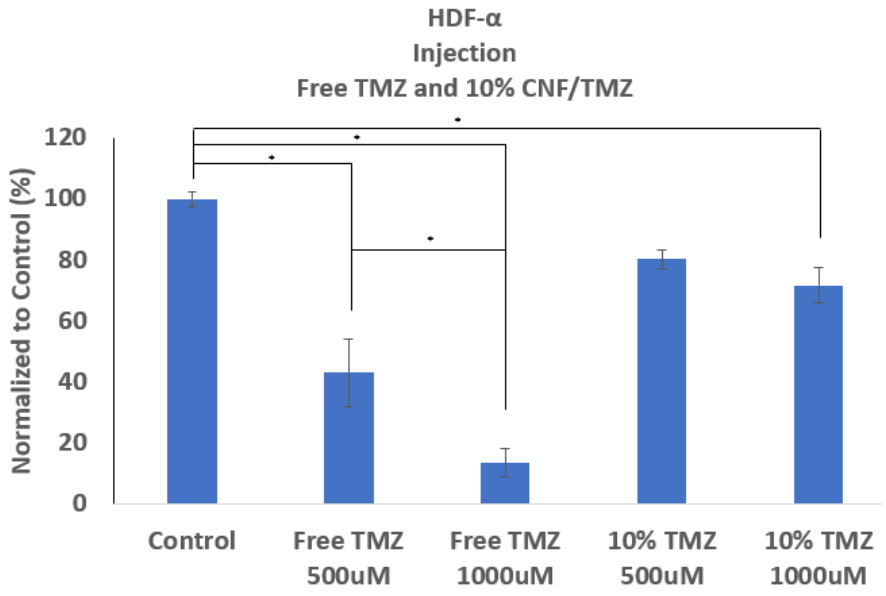

*Figure 21: **HDF-α cell viability using injection delivery of hydrogel loaded with TMZ:** HDF-α cells were seeded into 3D collagen matrices in 96 well plates and treated with either free TMZ or TMZ loaded into 10% CNF at concentrations of 500 and 1000uM using an injection method into the center of the collagen. Samples were left to incubate for 48 hours and then an MTS assay was performed to evaluate cell viability. Results were normalized to the control group.*

3.3.6 **Effect of cell death activators and inhibitors on DM6 cell viability with treatment**

Significant differences were seen between CNF/TMZ and CNF/TMZ + Glu ($p = 0.0067$) indicating that supplementation with glutathione was able to recover a majority of the cell death incurred by the CNF/TMZ treatment. Initial indications suggest that either CNF/TMZ directly

depletes glutathione levels by means of interfering with glutathione synthesis or availability of its amino acids, or a significant ROS expression occurs and GSH production is incapable of keeping up resulting in cell death due to oxidative stress. No difference was seen between CNF/TMZ and CNF/TMZ + Z-VAD-FMK indicating that the apoptosis inhibitor was unable to rescue the cells and that the cells are not undergoing caspase-dependent apoptosis. The addition of the ferroptosis inhibitor DFO with CNF/TMZ was also not able to rescue the cells indicating that excess iron accumulation is not occurring, and since there was a significant difference between CNF/TMZ and CNF/TMZ + DFO ($p = 0.011$) resulting in the addition of DFO causing more cell death it could be inferred that DFO acted upon basal levels of iron resulting in a synergistic toxic effect. As with prior cell viability tests there remained a significant difference between control and CNF/TMZ ($p=<0.0001$) and FT and CNF/TMZ ($p=0.001$).

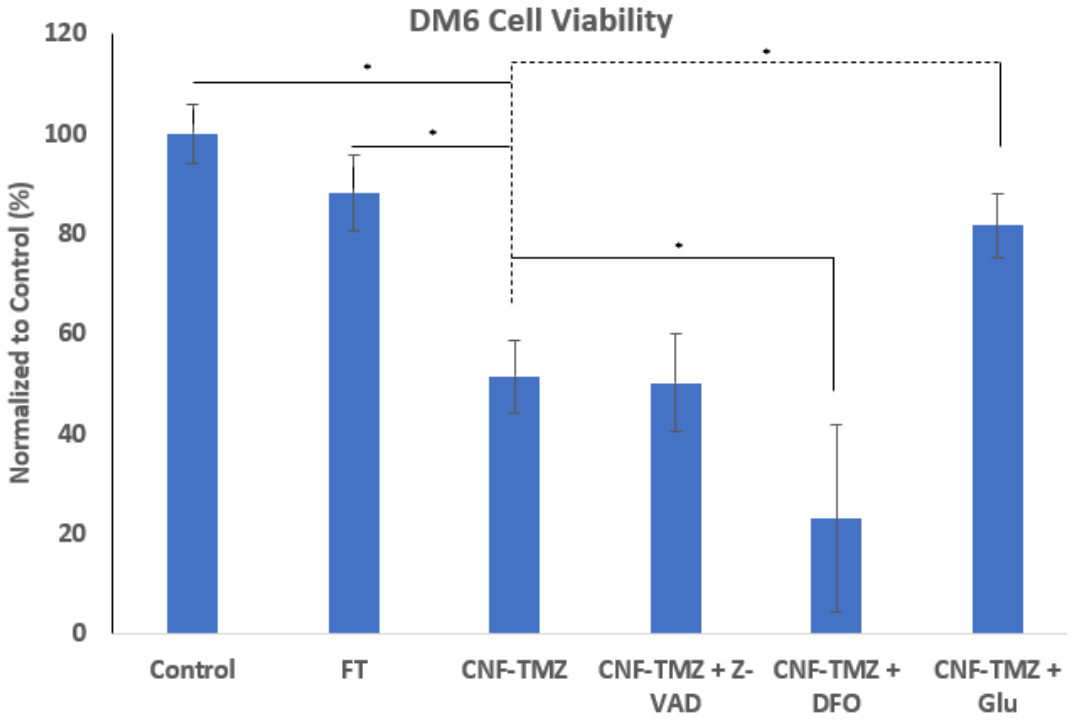

Figure 22: ***DM6 cell viability panel 1:*** *DM6 cells were seeded at 5,000 cells/well and allowed to incubate for 24 hours. After 24 hours treatments were added, and incubation occurred for a further 48 hours. Concentrations used were; FT (250uM, CNF-TMZ (250uM), Z-VAD-FMK (10uM), DFO (100uM), and Glu. Suppl. (5mM). Cell viability was determined by MTS assay.*

HDF-α cells showed recovery from FT with the addition of Z-VAD-FMK (p = <0.0001), an indication that when treated with FT HDF-α undergo caspase-dependent apoptosis. GSH supplementation was also able to rescue cells that were treated with FT (p = <0.0001), indicating a role for oxidative stress in the induction of apoptosis when treated with FT. No significant difference was found between CNF/TMZ and CNF/TMZ + Z-VAD-FMK or CNF/TMZ + Glu. Treatment with CNF/TMZ appears to not caspase-dependent or GSH-restrictive cell death.

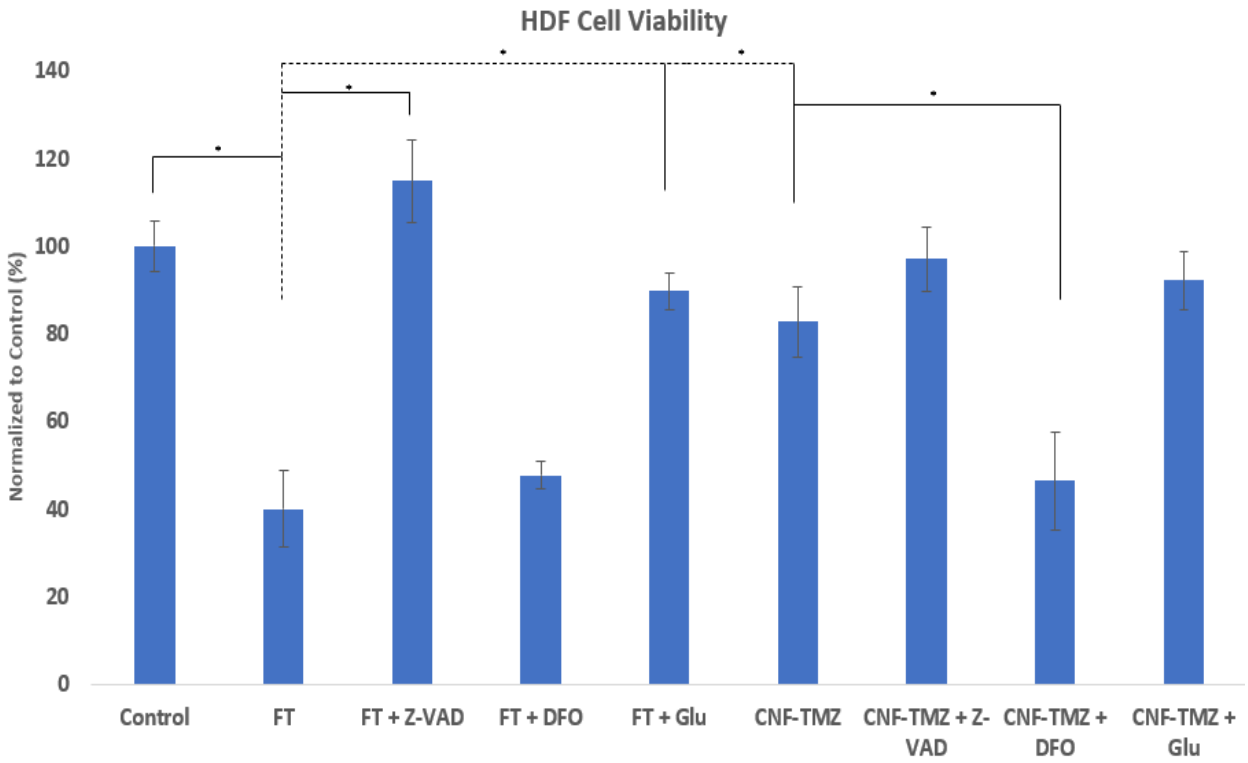

*Figure 23: **HDF-α cell viability panel 1:** HDF-α cells were seeded at 5,000 cells/well and allowed to incubate for 24 hours. After 24 hours treatments were added, and incubation occurred for a further 48 hours. Concentrations used were; FT (250uM, CNF-TMZ (250uM), Z-VAD-FMK (10uM), DFO (100uM), and Glu. Suppl. (5mM). Cell viability was determined by MTS assay.*

Treatment with BSO shows a significant decrease in cell viability relative to the control (p = 0.0128) indicating that inhibition of GSH synthesis can cause minor cell death in DM6. No significant difference was seen between Erastin and RSL3 treatment in respect to the control

group, indicating ferroptosis is not occurring and inhibition of cystine import and GPX4 activity does promote cell death. Further confirmation that DM6 cell death is not because of ferroptosis comes from the fact that ferrostatin-1 does not rescue CNF/TMZ treated cells. It also appears that there is no synergistic effect when BSO and CNF/TMZ are combined. Combined with the data that GSH supplementation rescues CNF/TMZ treated cells, yet combined treatment with BSO does not cause more cell death it appears that CNF/TMZ could act in a similar manner as BSO regarding GSH synthesis inhibition.

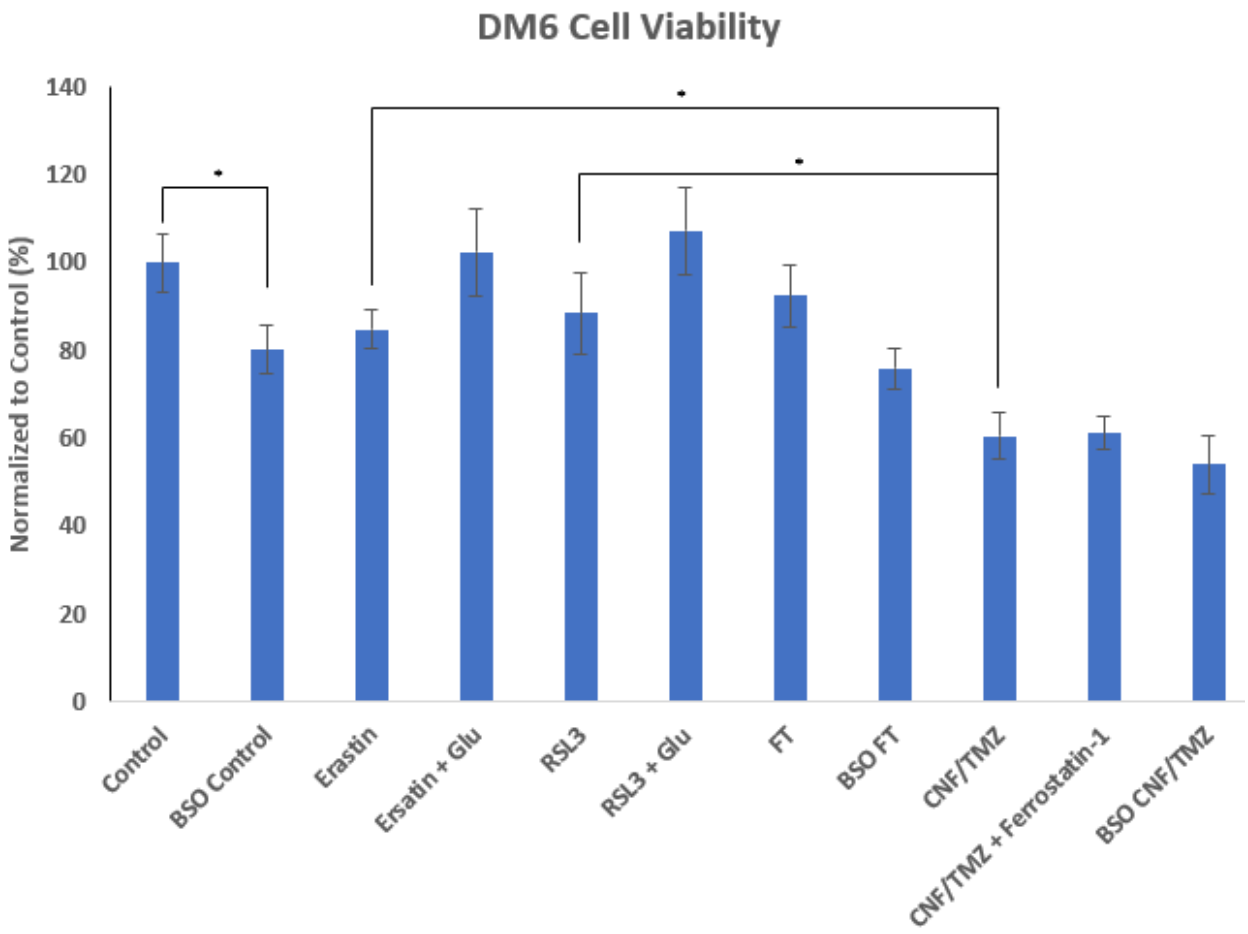

*Figure 24: **DM6 cell viability panel 2:** DM6 cells were seeded at 5,000 cells/well and allowed to incubate for 24 hours. After 24 hours treatments were added, and incubation occurred for a further 48 hours. Concentrations used were; FT (250uM, CNF-TMZ (250uM), BSO (100uM), Erastin (8uM), RSL3 (0.5uM), Ferrostatin-1(8uM), and Glu. Suppl. (5mM). Cell viability was determined by MTS assay.*

HDF-α cell viability was drastically reduced with the addition of BSO to CNF/TMZ compared to control (p = <0.0001). BSO is known to be highly toxic to healthy tissue, a determining factor in the reason it is not highly considered a viable treatment for cancer. This could reason that CNF/TMZ treatment alone does not influence intracellular GSH levels to an extent to be lethal.

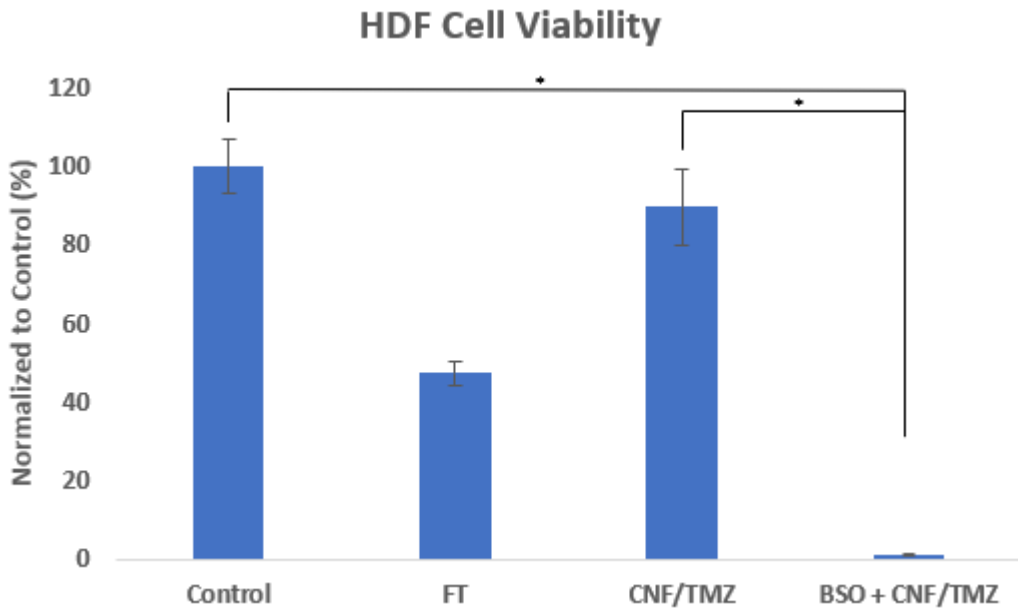

*Figure 25: **HDF-α cell viability panel 2:** HDF-α cells were seeded at 5,000 cells/well and allowed to incubate for 24 hours. After 24 hours treatments were added, and incubation occurred for a further 48 hours. Concentrations used were; FT (250uM, CNF-TMZ (250uM), and BSO (100uM). Cell viability was determined by MTS assay.*

Based on the results seen with BSO on DM6 cell viability a test with increasing dosages was needed to determine if there could be any synergistic effect with either FT or CNF/TMZ. We saw that GSH supplementation rescued CNF/TMZ treated DM6 and BSO alone does promote cell death, so I wanted to find an optimal dose of BSO to act as a known GSH inhibitor that has a lethal effect for downstream experiments that will include analysis of GSH-related molecules. 1000uM of BSO showed a significant drop in cell viability when compared to control (p = <0.0001) and FT (p = 0.001), but not with CNF/TMZ. Because of this I cautiously assume that at this concentration there could be some off-target cytotoxicity, so I did not use this

concentration in further experiments. BSO at a concentration of 250uM showed to significant different with either control or FT, but it did with CNF/TMZ ($p = 0.0156$) possibly indicating further suppression of GSH.

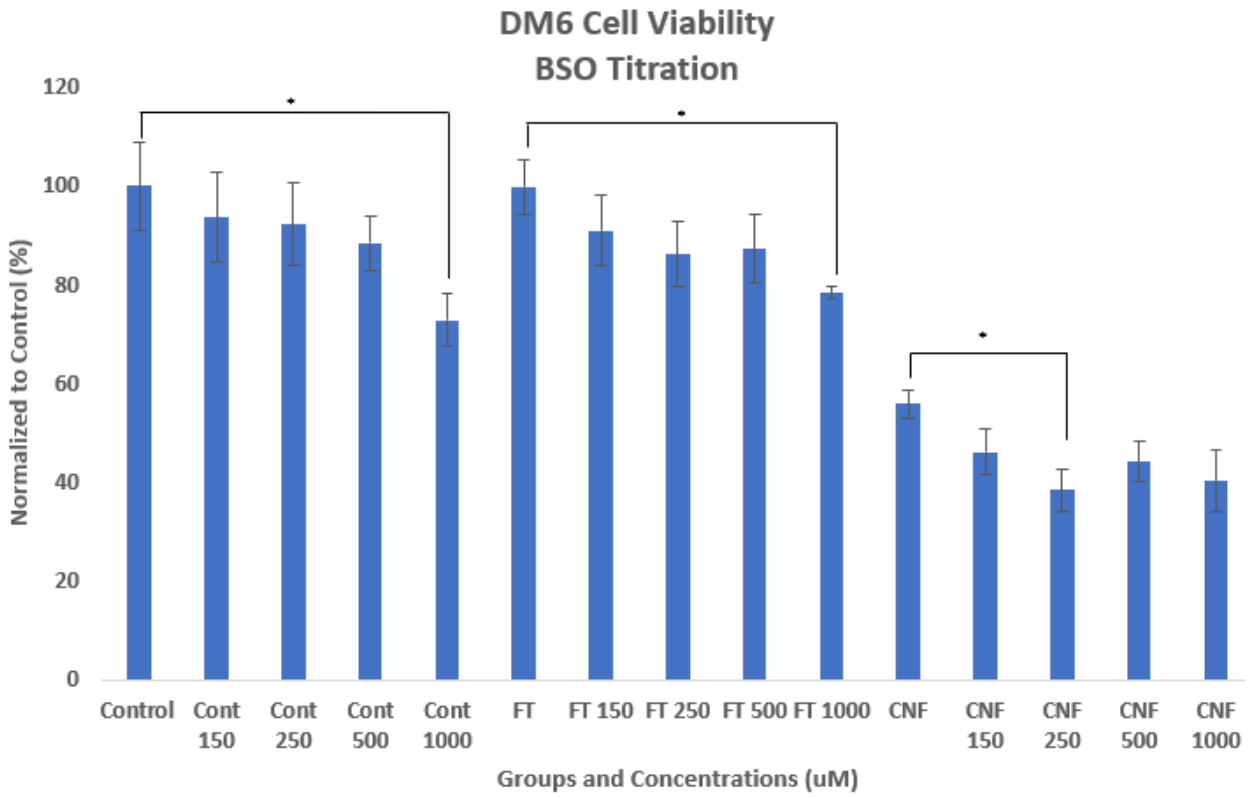

Figure 26: ***BSO dosage test:*** *DM6 cells were seeded at 5,000 cells/well and allowed to incubate for 24 hours. After 24 hours treatments were added, and incubation occurred for a further 48 hours. Concentrations used were; FT (250uM and CNF-TMZ (250uM). BSO was supplied 16 hours before other treatments at the labeled dosages. Cell viability was determined by MTS assay.*

3.4 Summary

Embedding cells in a 3D collagen matrix requires an increase in the concentration of TMZ required. Using a 3D matrix also allows for delivery methods that are more replicable of the proposed clinical applications which are intratumoral injection and topical spreading. DM6 cell viability differed between free TMZ and 10% CNF at the higher concentration of 1000uM. The most dramatic results were that 10% CNF at 1000uM proved to be much safer for HDF-α cells

compared to free TMZ 1000uM. 10% CNF loaded with drug X exhibited a slight significant difference at 2.5uM concentration, but overall, no difference was seen between free drug x and 10% CNF. We can conclude that modified CNF increases the efficiency of TMZ cytotoxic effects on DM6 due to its ability to stabilize and prolong the release of TMZ which requires the maintenance of a more acidic pH within the hydrogel for TMZ stability. Cell viability assays of melanocytes and keratinocytes to 10% CNF-TMZ and free TMZ remains to be performed. Confirmation of MTS assays will be done with Hoechst and PI staining. Cell viability when hydrogel is administered in a topical method will be conducted.

Caspase-dependent apoptosis seems to be the cause of HDF-α cell death when treated with FT, as cell viability was retained when treated with Z-VAD-FMK, but no ability to rescue cells was seen in DM6 when DM6 was treated with CNF/TMZ.

The initial hypothesis of cell death mediated by ferroptosis in DM6 was found to be false, indicated by the inability to cause significant cell death with the ferroptosis activators Erastin and RSL3, as well as an inability to rescue cells with ferroptosis inhibitors ferrostatin-1 and DFO. While iron accumulation caspase-dependent apoptosis may not play a role in DM6 cell death it does appear that GSH reduction in some fashion does, as GSH supplementation was able to rescue both DM6 and HDF-α when they were a treatment caused significant cell death. The method behind what is causing inadequate GSH within the cell will be the next thing to decern, but the results in this aim have provided a good place to begin looking.

Chapter 4: Aim 3: Depletion of chemoresistance molecules reduces DNA damage response and increases oxidative stress

4.1 Introduction

Cancer cell chemoresistance is the root cause of most cancer resurgences after treatment. Without proper treatment cancer cells can adapt to therapies rendering that therapy useless or requiring higher dosages, potentially causing damage to healthy tissues. Melanomas are derived from melanocytes, and cell derived for melanocytes exhibit a higher sensitivity to ROS increases. This has resulted in melanomas needing to rely on efficient antioxidant measures in order to retain a beneficial level of ROS and not crossing over to a lethal level [75]. Cancer cells in general typically have higher basal levels of ROS production and antioxidant production, primarily GSH. Melanomas are no different. This increase in ROS seems to primarily result from mitochondrial uncoupling and dysfunction. NADPH oxidase (NOX) family, nitric oxide synthase (NOS) uncoupling, peroxisomes, and melanosomes are also thought to promote increased ROS generation in melanoma cells.

It is generally thought that are two main methods of causing cancer cells to surpass the lethal limit of oxidative stress, one being further increasing ROS production to a point where antioxidant relief measures cannot keep up, and the second is to cause depletion of antioxidant, primarily GSH, in hopes that this will allow the elevated ROS to run rampant causing cell death. Research into therapeutic measure that further increase ROS production in hopes of surpassing the lethal limit at which antioxidant are gaining in popularity. The drug wortmannin sensitizes melanomas to TNF-related apoptosis-inducing ligand (TRAIL) mediated apoptosis through ROS-dependent phosphorylation of Bax. NOX inhibitors such as Diphenyliodonium (DPI) have

shown to be effective in killing on melanoma cells in vitro but do to its high toxicity and non-specificity its use as a clinical treatment is limited [76].

Combinatory treatments that include a GSH inhibitor, primarily BOS, are being studied and have shown to enhance the killing effect of several platinum-based chemotherapy agents including cisplatin and iproplatin. BSO acts on GSH through inhibition of γ-glutamylcysteine synthetase (GCS) irreversibly. GCS is the catalyst for the first metabolic step of glutathione synthesis. Interestingly, BSO on its own does not demonstrate significant cytotoxicity even though it is capable of depleting GSH by as much as 91% within 48 hours. GSH has shown to influence iproplatin treatment, likely by its effects on DNA repair and ROS scavenging [74, 77-79].

Erastin is a ferroptosis inducing drug. Ferroptosis is a form of cell death that is reliant on the accumulation of labile iron and ROS production resulting in lipid peroxidation of the cell membrane ultimately causing leakage to occur resulting in cell death. Erastin has been shown to induce ferroptosis through inactivation of SLC7AA, the primary glutamate/cystine antiporter resulting in the depletion of GSH and loss of cellular redox homeostasis. Erastin has been shown to inhibit the growth of A372 melanoma cell lines [80].

GSH play numerous roles in the chemoresistance of cancers and I highly upregulated due to higher levels of ROS production and increases in gene expression for proteins involved in GSH synthesis such as nuclear factor, erythroid 2-related factor (Nrf2). GSH within DNA damage response pathways, binds and deactivates electrophiles, and its traditional role as an ROS scavenger to maintain redox homeostasis. GSH activity also includes the regeneration fo glutathione peroxidases (GPXs) that are responsible for lipid hydroperoxide detoxification. In

combination with GST, GSH is capable of detoxifying xenobiotics, including alkylating agents [81].

GSH exists in two states: the thiol or reduced for (GSH) and disulfide or oxidized form (GSSG). GSSG is produced as GSH reduced H_2O_2 into water in a selenium-dependent manner. GSSG can then be reduced through the use of $NADPH^+$ and glutathione reductase to form GSH, or alternatively be imported out of the cell causing depletion of GSH [81]. The GSH/GSSH ratio is an important indication of oxidative stress levels. Lower levels of the GSH/GSSG ratio are associated with higher oxidative stress as the increase in GSSH is likely the result of GSH being oxidized in order to detoxify increased ROS. Attempts at shifting the ratio of GSH:GSSG towards a more oxidized state has been shown to be effective at inducing apoptosis in melanoma cells [82]. This was achieved using disulfiram (DSF), which is now in clinical phase I/II studies in human metastatic melanoma (NCT00256230). Further, the combination of melphalan and BSO, an irreversible inhibitor of γ-glutamylcysteine ligase (GCL), is being evaluated for use in patients with persistent or recurring stage III malignant melanoma (NCT00661336)

O6-methylguanine-DNA methyltransferase (MGMT) acts as a DNA "suicide" repair enzyme in response to alkylating agents. MGMT is known to be the primary regulator of chemoresistance to TMZ in glioblastomas. MGMT is capable of repairing methylated guanine nucleotides by transferring the methyl group at the O6 site of guanine to its cysteine residues, ensuring the cell avoids gene mutation and cell death [83]. Reduction or methylation of MGMT promotes sensitivity to alkylating agents. A potential method of reduction is the reduction of intracellular cysteine or methionine levels, meaning that inhibition of SLC7A11 or the Transsulfuration pathway could acts as a limiting factor in MGMT production [84].

Nrf2 is a key transcription factor that regulated the expression of antioxidant proteins by binding to antioxidant response elements (AREs) in the nucleus leading to transcription of ARE genes. Nrf2 is localized to the cytoplasm by Kelch like ECH-associated protein 1 (KEAP1) which degrades Nrf2 by ubiquitination, where it is then transported to the proteasome and degraded and recycled. In times of oxidative stress Nrf2 dissociates from KEAP1 and levels begin to elevate within the cytoplasm before translocating into the nucleus. Important GSH synthesis proteins are regulated by transcriptional activity of Nrf2 with their respective genes. This includes glutamate-cysteine ligase regulatory subunit (GCLM) and glutamate-cysteine ligase catalytic subunit (GCLC), establishing Nrf2 as an important regulator of GSH synthesis. Nrf2 also regulates GST levels, meaning Nrf2 has a role in the xenobiotic detoxifying ability of GSH when acting in tandem with GST [85, 86]. Elevated levels of glutathione S-transferase along with GSH can increase the rate at which GSH conjugates with chemotherapy agents, reducing their cytotoxic effects [87]. Further, Nrf2 acts as a primary regulator of SLC7A11 expression. SLC7A11 is an antiporter that is primarily responsible for the intake of cystine to be made into cysteine for GSH synthesis. It does this at a 1:1 of export:import with glutamate and cystine. Cells that have weak endogenous cysteine production primarily rely on this importation to generate GSH, as cysteine is the rate limiting factor in GSH synthesis [88] . The expression of SLC7A11 has been shown to be much higher in melanoma patients than in healthy patients, possibly indicating an important role for SLC7A11 in redox homeostasis [89]. Disruption of SLC7A11 resulting in the loss of activity in highly metastatic B16F10 mouse melanoma cells promoted cell death and increase survival rates in mice [90].

Cystathionine acts as an intermediate in the synthesis of endogenous cysteine via the Transsulfuration pathway. Cystathionine is broken down into cysteine, α-ketobutyrate, and

ammonia by cystathionine γ-lyase (CTE and cystathionase). It is the rate limiting substrate in the synthetic pathway for GSH synthesis in several tissues. Elevated ROS target CTE resulting in oxidized cystathionase and decreasing its activity. This decrease in activity then lowers intracellular cysteine, resulting in lowered levels of GSH and increased oxidative stress. Deficiencies in cystathionase activity have been shown to contribute to glutathione depletion in cancer patients [91]. Nrf2 transcriptionally upregulates cystathionine β-synthase (CBS), an enzyme responsible for the catalysis of homocysteine to cystathionine in the first step of the Transsulfuration pathway [92, 93]. The Transsulfuration pathway is a biochemical mechanism that allows for the endogenous production of cysteine, which can used downstream in GSH synthesis. It utilizes methionine metabolism for the biosynthesis of cysteine, glutathione, and taurine. Deficiencies in the enzymes that make up the pathway induce increased ROS production, homocysteine accumulation, and further contributions to tumorigenesis [94].

4.2 Experimental Section

4.2.1 **Oxidative stress measurements**

DM6 and HDF-α cells were seeded at 5,000 cells/well and allowed to attach for 24 hours. BSO (250uM) was added 16 hours prior to the addition of the other treatments. The Promega ROS-Glo H_2O_2 assay was used in this experiment. 6 hours before the end of the 48-hour incubation H_2O_2 substrate (supplied with the assay) was added to each well as well as 3 extra wells to serve as a blank. 30 minutes prior to performing the assay H_2O_2 (500uM) was added to the respective group to serve as a positive control. After 48 hours of incubation the ROS-Glo detection solution was added, and the cells were incubated for 20 minutes at room temperature. All samples were then transferred to a white luminescence 96 well plate for analysis. Analysis was performed using

a spectrophotometer and measuring the relative luminescence. ROS levels were then normalized to the respective control group.

4.2.2 **Antioxidant level measurement**

DM6 and HDF-α were plated at 5,000 cells/well and allowed to attach for 24 hours. Duplicates of all groups were plated to allow for the measurement of total GSH and GSSG, as each measurement needs its own samples. BSO (250uM) was added 16 hours prior to the addition of other treatments. After 24 hours cells were treated with the respective treatments and incubated for a further 48 hours. After 48 hours total GSH and GSSG were measure using the Promega GSH/GSSG-Glo Assay. After all reagents were prepared the old media was removed, the cells were washed with PBS twice, and then lysed with the supplied buffers and 3 wells were added as blanks, then gently shaken for 5 minutes. Luciferin generation reagent was then added to each well, including blanks and incubated at room temperature for 30 minutes. Luciferin detection reagent was then added and allowed to equilibrate for 15 minutes at room temperature. Luminescence was then read using a spectrophotometer. The GSH:GSSG ratio was then calculated based on the relative luminescence units (RLU) and the following equation:

$$\textbf{Control group} = \frac{\textbf{(Net vehicle total GSH RLU – Net vehicle GSSG RLU)}}{\textbf{(Net treated GSSG RLU/2)}}$$

$$\textbf{Treated groups} = \frac{\textbf{(Net treated total GSH RLU – Net treated GSSG RLU)}}{\textbf{(Net treated GSSG RLU/2)}}$$

GSSG results are divided by 2 to reflect the number of moles of GSSG in the sample, as the signal from one mole of GSSG is equal to the signal from two GSH.

4.2.3 **Western blot analysis**

Cell treatment was performed as normal for 48 hours, at which point the cells were lysed using Trypsin for 5 minutes. Equal parts of 10% RPMI media were added to each well to neutralize the trypsin and the cells were collected and counted using trypan blue. They were then spun down at 1,500 RPM for 5 minutes. The supernatant was removed, and the cells were washed with PBS, then spun down again. After removing the supernatant RIPA buffer with protease inhibitor was added (amount based on number of cells counted) and incubated on ice for 30 minutes. The cell solution was then briefly sonicated at low power and spun down at 12,000g for 15 minutes at 4°C. Finally, the supernatant was removed, and protein quantification was done using a BCA assay. Once the protein was quantified the sample was aliquoted into 20ug samples and stored at -20°C.

For western blot the samples were prepared by adding Laemmli buffer at a 1:4 ratio and heated at 95°C for 5 minutes. The samples were then kept on ice until cool and spun down to drag any condensation back into the sample. Electrophoresis was prepared with BioRad stain free gels and fresh running buffer that had been stored at 4°C. Samples were loaded into the gel at 18uL quantities along with 7uL of ladder. The gel was run at a constant voltage of 50V for 5 minutes to compact the samples and then 100V for 1.5 hours. The gel was then imaged for total protein quantification and then transferred onto a nitrocellulose membrane using a turboblot and a 10-minute transfer setting. After transfer the gel was imaged again to ensure complete transfer and the blot was also imaged using stain free imaging. A 5% milk solution made of powdered milk and TBST was used for blocking, which was done for 1 hour at room temperature with gentle rocking. After blocking the gel was washed with TBST 3X for 5 minutes each. The primary antibody was added in a 1% milk solution at the recommended dilution and allowed to

incubate overnight at 4°C with gentle rocking. The blot was then washed with TBST 3X for 5 minutes each while rocking before the secondary antibody in 1% blocking solution was added. The secondary antibody was incubated at room temperature for 2 hours with gentle rocking. The blot was then washed with TBST 3X for 5 minutes each while rocking and then the ECL reagent was added at a 1:1 dilution for 5 minutes. Finally, the blot was imaged using a chemiluminescence imager to get the bands and then imaged using the colorimetric setting to get the ladder. The two images were then merged. ImageJ was used to calculate the intensity of the total protein stain to ensure equal loading of all lanes and of the blot to quantify and normalize the bands to the control group.

4.3 Results and Discussion

4.3.4 **Intracellular ROS assay**

Significant differences in ROS expression in DM6 cells were seen between the CNF/TMZ group and the control group ($p = 0.0009$), FT group ($p = 0.0063$), Erastin group ($p = 0.0003$), and BSO group ($p = 0.0001$). Surprisingly, not ROS increase was seen with either Erastin or BSO, both know to promote GSH depletion.

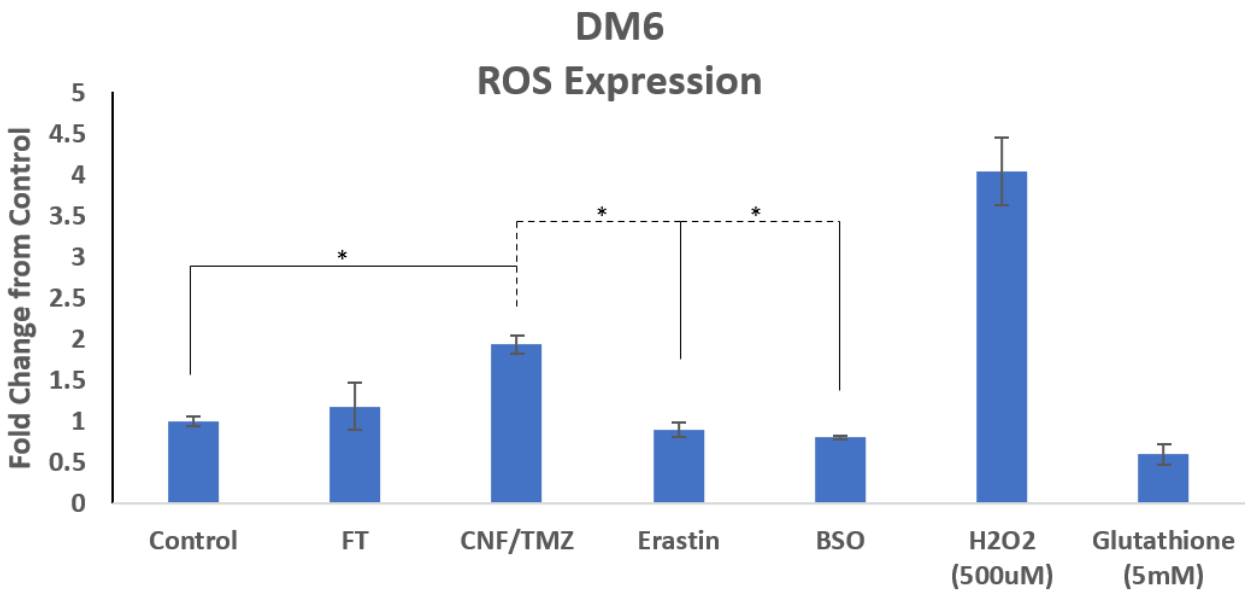

Figure 27: ***DM6 ROS Expression:*** *ROS levels were measured with a ROS-Glo kit, using H_2O_2 as a positive control. Cells were seeded at 5,000 cells/well and treated for 48 hours. BSO was added 16 hours prior to all other treatments being applied.*

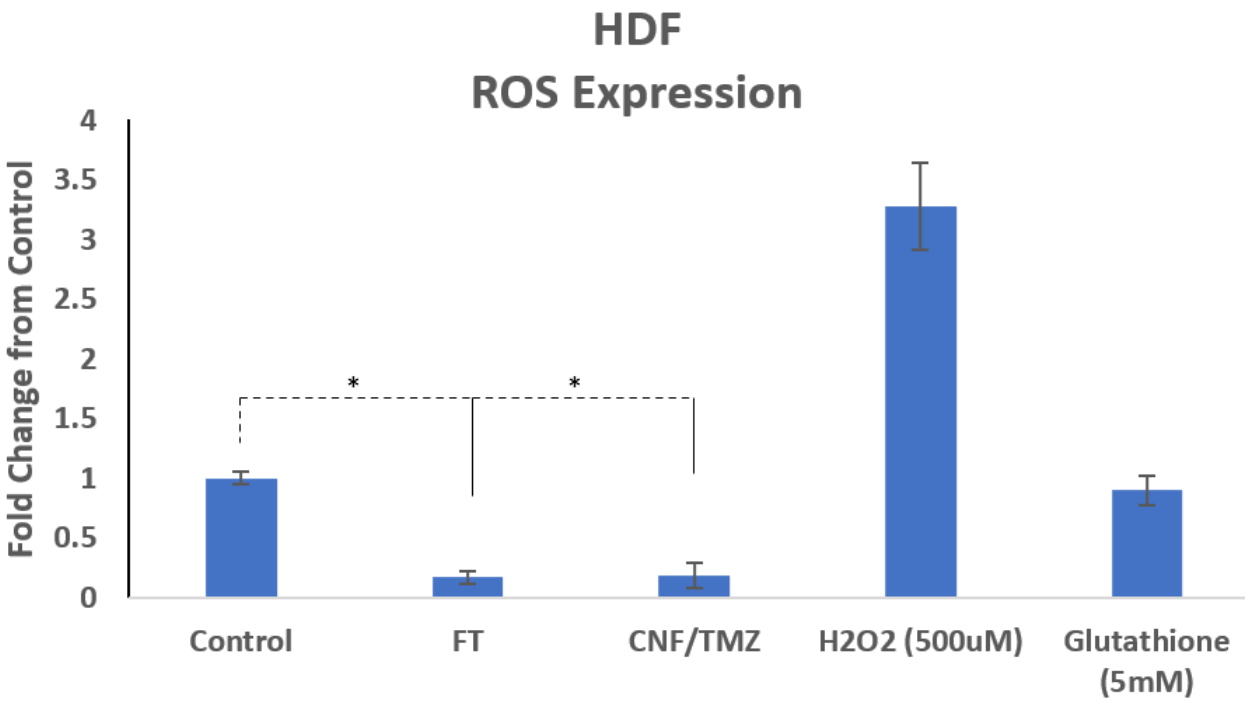

Figure 28: ***HDF-α ROS Levels:*** *ROS levels were measured with a ROS-Glo kit, using H2O2 as a positive control. Cells were seeded at 5,000 cells/well and treated for 48 hours. BSO was added 16 hours prior to all other treatments being applied.*

4.3.5 **Total Glutathione Levels and Glutathione/Glutathione Disulfide (GSSG) Ratio**

Total GSH levels in the HDF-α for both treatment groups were depleted relative to the control, with FT being depleted to a much more significant level. Significance was shown between the control group and FT ($p = 0.0053$) and control and CNF/TMZ groups ($p = 0.0311$). Significance was also seen between FT and CNF/TMZ ($p = 0.0453$). Cell viability results had shown that FT caused a much more significant loss of viability to HDF-α cells, while CNF/TMZ did not show significant losses, but there was some cell death. Along with the Z-VAD-FAK and GSH supplementation cell viability data it is reasonable to say that GSH depletion appears to promote apoptosis, at least in part, in HDF-α cells with FT doing it to a highly significant degree.

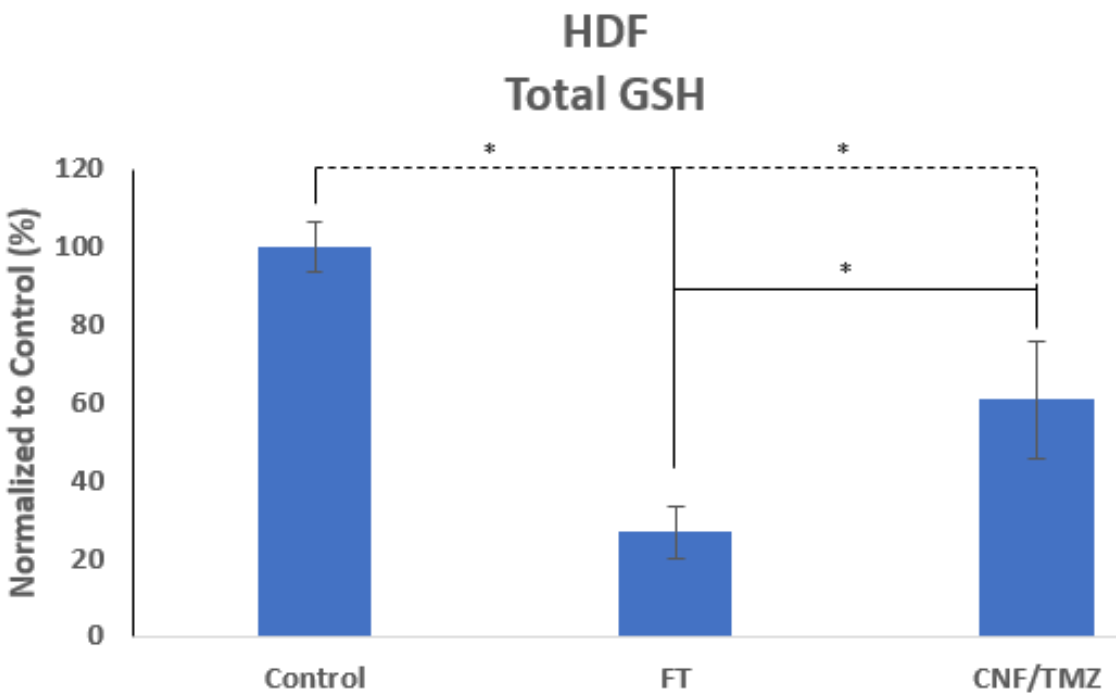

Figure 29: ***Total Intracellular GSH HDF-α:*** *Total GSH levels were measured in HDF-α cells after 48 hours of treatment. Cells were seeded at 5,000 cells/well and treated with 250uM of TMZ either as a free drug or loaded into CNF. GSH levels were then detected using a ROS luminescence assay kit.*

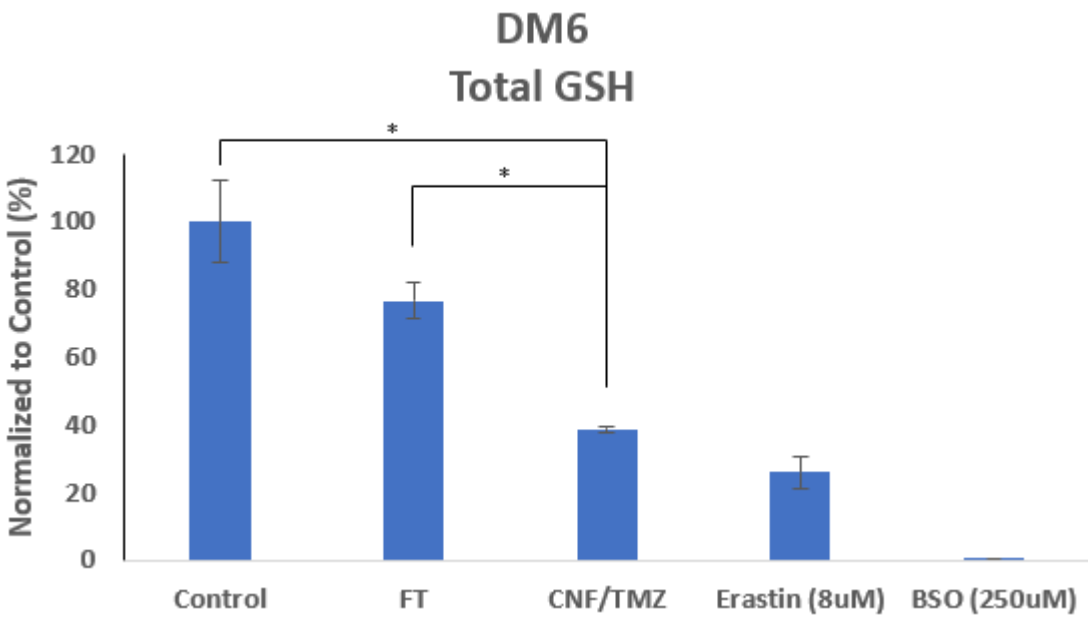

Figure 30: ***Total Intracellular GSH DM6:*** *Total GSH levels were measured in DM6 cells after 48 hours of treatment. Cells were seeded at 5,000 cells/well and treated with 250uM of TMZ either as a free drug or loaded into CNF. BSO was added to its respective group 16 hours prior to TMZ and Erastin treatments being added. GSH levels were then detected using a ROS luminescence assay kit.*

When treated with CNF/TMZ DM6 showed a significant depletion of total GSH relative to the control group ($p = 0.0008$) and the FT group ($p = 0.0069$). BSO showed a high level of GSH depletion, which makes sense given that BSO is an irreversible GSH synthesis inhibitor so the initial supply of GSH would be inhibited and would fail to be able to replenish itself. An interesting observation is that Erastin maintained similar levels to CNF/TMZ. This might indicate that either cystine import is still somewhat functional or that DM6 is able to produce endogenous cysteine through the Transsulfuration pathway to maintain GSH synthesis to some degree

Low GSH/GSSG ratios alongside low levels of GSH levels are considered indications of oxidative stress. Our results show that relative to the control group the CNF/TMZ group had a significantly lower GSH/GSSG ratio, indicating that GSH was being consumed and oxidized into

GSSG more rapidly than GSSG could be reverted into GSH. No significant difference was found between Erastin and CNF/TMZ groups, possibly indicating a similar mechanism of action. It is also possible that a portion of the GSH pool is being utilized alongside glutathione S-transferase to bind to TMZ molecules and deactivating its cytotoxic ability.

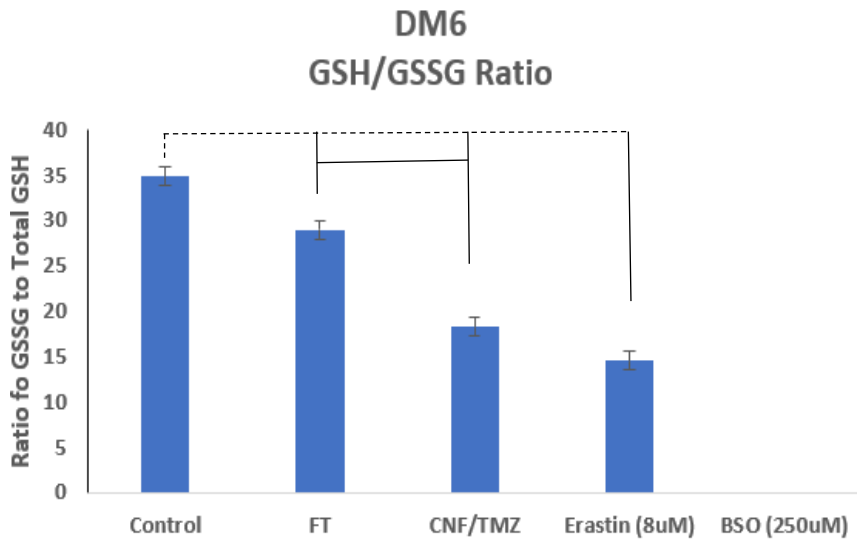

*Figure 31: **DM6 GSH/GSSG ratio:** GSH:GSSG ratio was measured by running two groups in parallel, measuring one for total GSh and the other for GSSG. We found that CNF/TMZ and Erastin both had a significant decrease in the ratio compared to control and free TMZ group. Lower ratios indicate oxidative stress, demonstrating, alongside the low total GSH levels, that CNF/TMZ is promoting an increase in oxidative stress.*

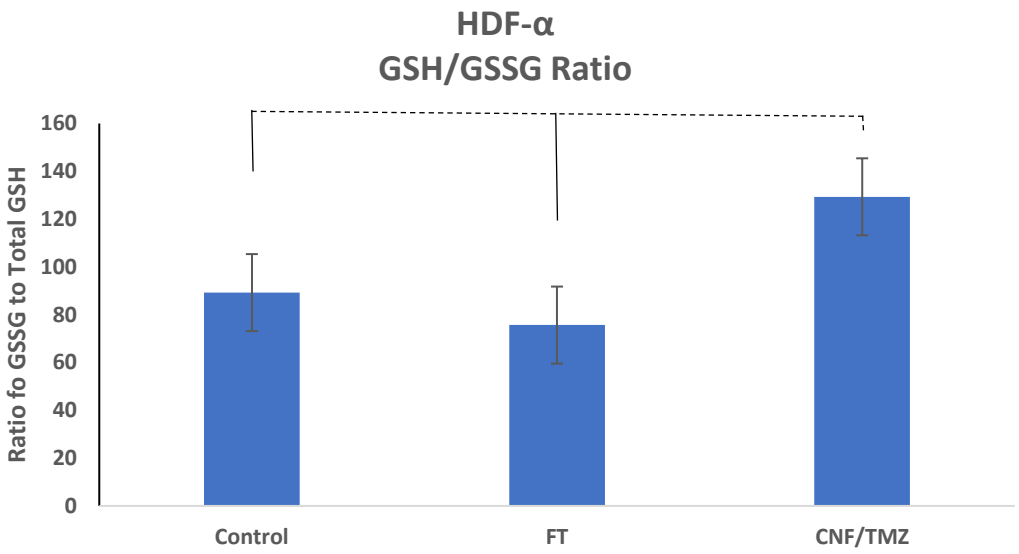

*Figure 32: **HDF-α GSH/GSSG Ratio:** Parallel groups were run and total GSH and GSSG levels were measured and then the ratio was calculated. A significant increase in ratio was seen in the CNF/TMZ group indicating a possible decrease in oxidative stress for that group.*

4.3.6 **MGMT Western Blot**

Significant MGMT reduction is see in CNF/TMZ treated DM6 and FT treated HDF-α relative to their respective control. Further, in both cell lines we see an increase over the control in their respective groups that do not cause significant cell death. In the case of DM6, these cells rely heavily on MGMT for repair of TMZ-induced DNA damage and prolonging that release severely depletes MGMT stores and there is not an adequate amount of time to restore intracellular levels. HDF-α when treated with FT sees even more severe depletion that DM6. These results are interesting because they demonstrate a significant difference in reaction to bulk drug delivery and a sustained, slow release of the same drug. When comparing the control groups between the two cell lines it is obvious that basal levels of MGMT are much higher in DM6. This could provide an immediate high response to bulk TMZ delivery, while HDF-α does not have the same capacity of repair in the quick of a time and ultimately succumbs to cell death.

It could be possible that with the slow release ultimately more of the drug is reaching either cell line and the melanoma is already at high basal levels of ROS, which can cause DNA damage, so there could be a constant need to repair and by using a slow release the cells are continuously bombarded and MGMT storage and production gets overwhelmed. Inversely, HDF-α have a much initial storage capacity that is not capable of dealing with an immediate large cytotoxic response, but also does not have to deal with the high rate of constant ROS production and DNA damage, so all the focus can be on preventing DNA damage over the long run with smaller burst of potential cytotoxic damage.

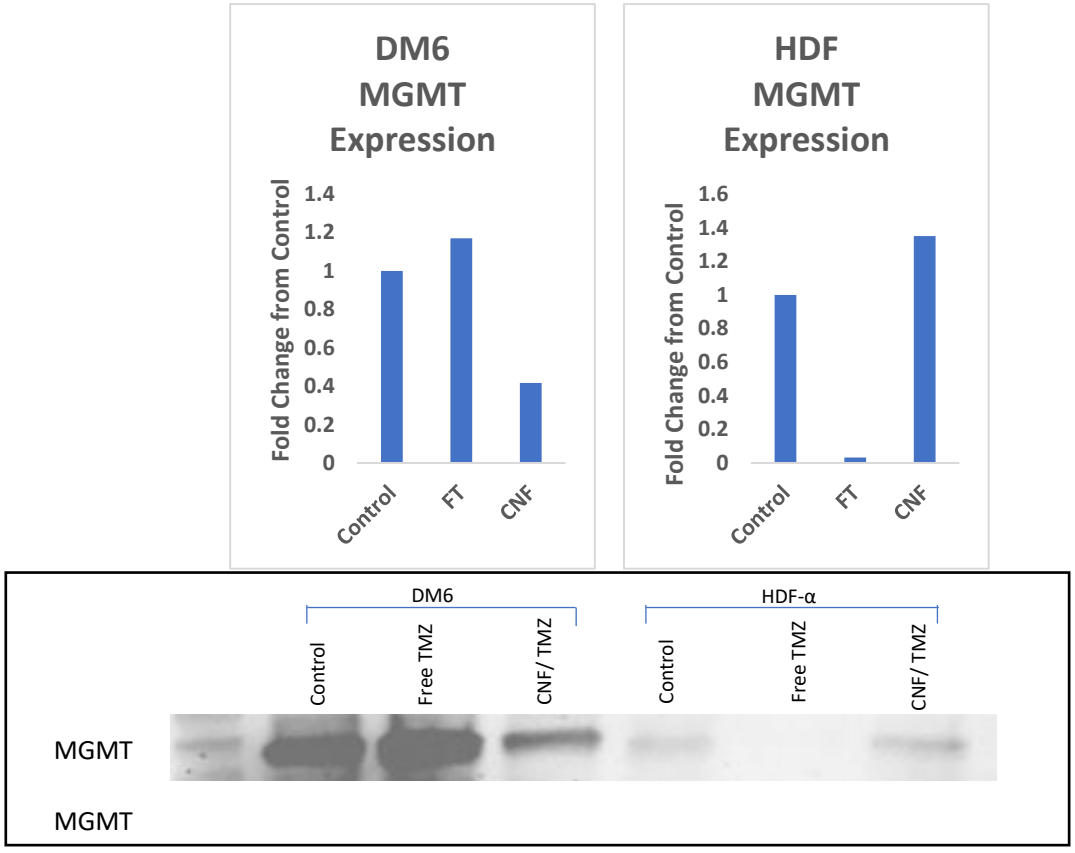

Figure 33: ***MGMT Expression:*** *MGMT expression is evaluated after 48 hours of treatment. Expression was increased in the free TMZ group and greatly reduced in the CNF/TMZ group in the DM6 cell line. Indication of MGMT depletion and reduced ability for methylated DNA damage repair. HDF-α cells saw severe reduced expression in the free TMZ group, and increased expression in the CNF/TMZ group indicating a role of MGMT for resistance in healthy cells.*

4.3.7 **Glutathione S-Transferase Western Blot**

Glutathione S-Transferase (GST) did not show any large moves in expression relative to the control in DM6 cells. One important usage of GST is to catalyze binding of GSH thiol groups to various electrophiles. TMZ being an alkylating agent is considered a high electrophilic compound and if GSH was being used as a deactivator I would expect to see higher levels in resistant DM6 treatment group, such as FT groups. While there is a slight increase in expression in the FT group its possible that GSH binding to TMZ for deactivating is a minor role in the resistance seen, but when the other proteins blotted for are viewed all together along with the significant increase in ROS, it seems more likely that GSH is utilized more in its traditional role as an antioxidant. However, in HDF-α cells we see a relatively large increase in expression in the CNF/TMZ group. HDF-α cells might be taking advantage of this protein's ability to assist in detoxifying TMZ.

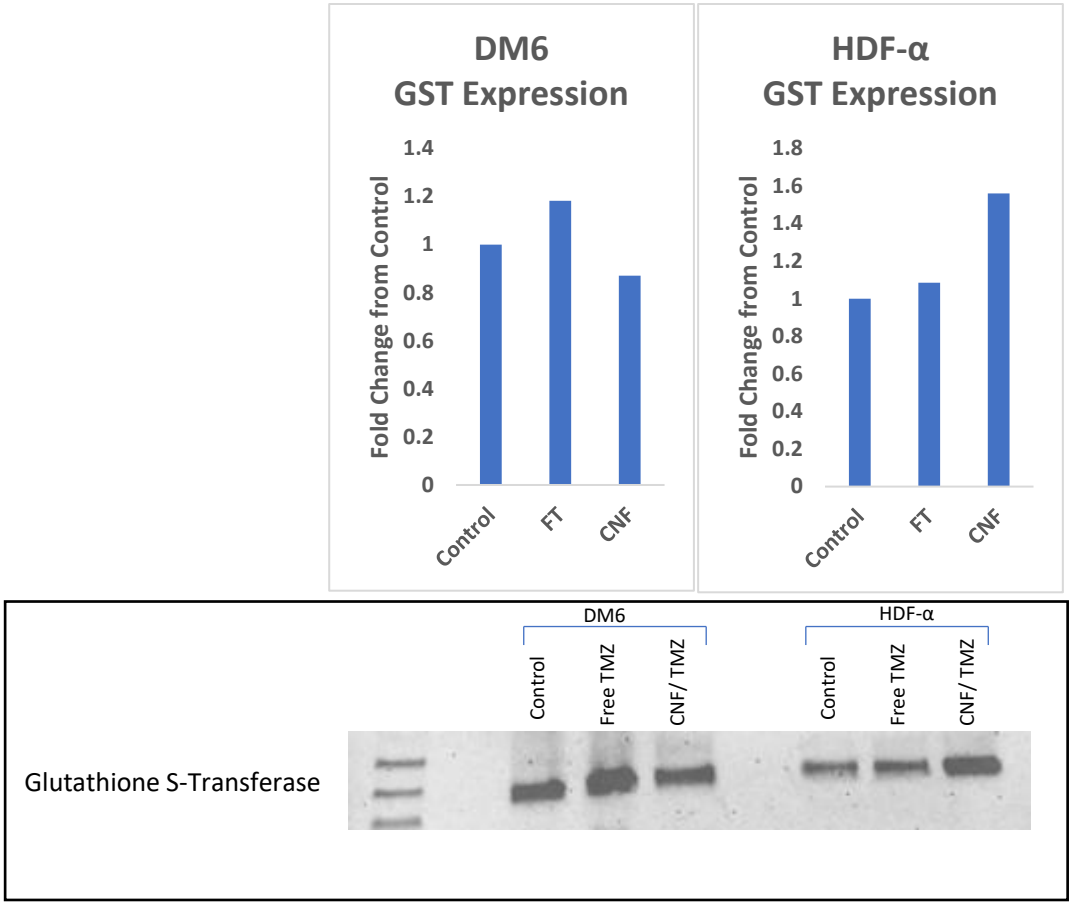

Figure 34: ***Glutathione S-Transferase Expression:*** *Western blot appears to show that glutathione S-transferase (GST) expression is useful for promoting chemoresistance, but depletion does not necessarily correlate with cell death. We see upregulation of GST in DM6 free TMZ and HDF-α CNF/TMZ, both groups that show no significant cell death. GST expression was not reduced in DM6 CNF/TMZ and HDF-α free TMZ groups where significant cell death does occur.*

4.3.8 **Nrf2 Western Blot**

DM6 treated with CNF/TMZ show a dramatic decrease in Nrf2 expression relative to control. In fact, it appears there is almost an undetectable amount. FT treated DM6 responds by upregulating the expression, meaning this protein is highly likely involved in the chemoresistance we see with FT treatment. Depletion of Nrf2 is likely to result in the downregulation of multiple genes associated with glutathione synthesis and oxidative response to stress.

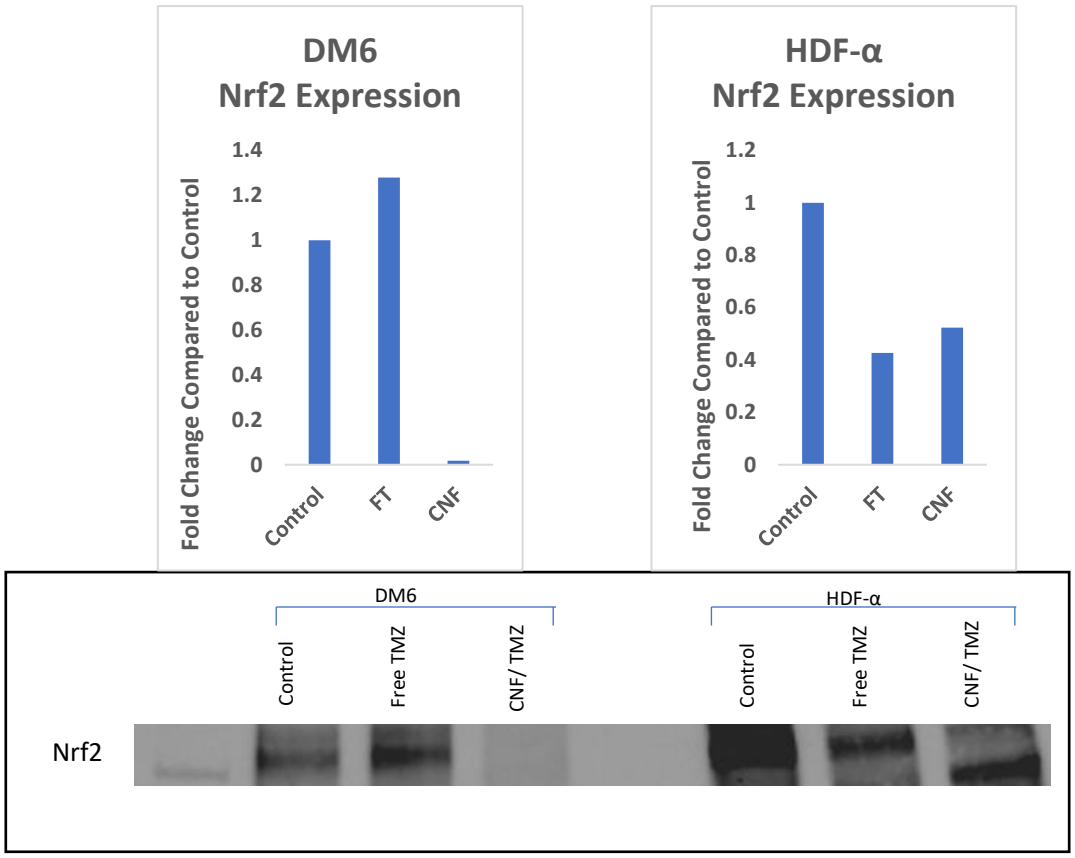

*Figure 35: **Nrf2 Expression:** Primary role of Nrf2 is transcriptional regulation of several antioxidant genes, and the downregulation of Nrf2 appears to promote cell death in DM6 cells, while lower levels are not an inherent cause of death in HDF-α. Severe decreased expression was seen in DM6 treated with CNF/TMZ, while upregulation was seen in the free TMZ group.*

4.3.9 **SLC7A11 Western Blot**

Falling into line with the reduction in Nrf2 we also see a steep drop in SLC7A11 levels after treating DM with CNF/TMZ. Interestingly there is a substantial increase in both FT and CNF/TMZ groups with the HDF-α groups. Decreased expression SLC7A11 means that reliance on other means of cystine are required as SLC7A11 is the primary antiporter for cystine.

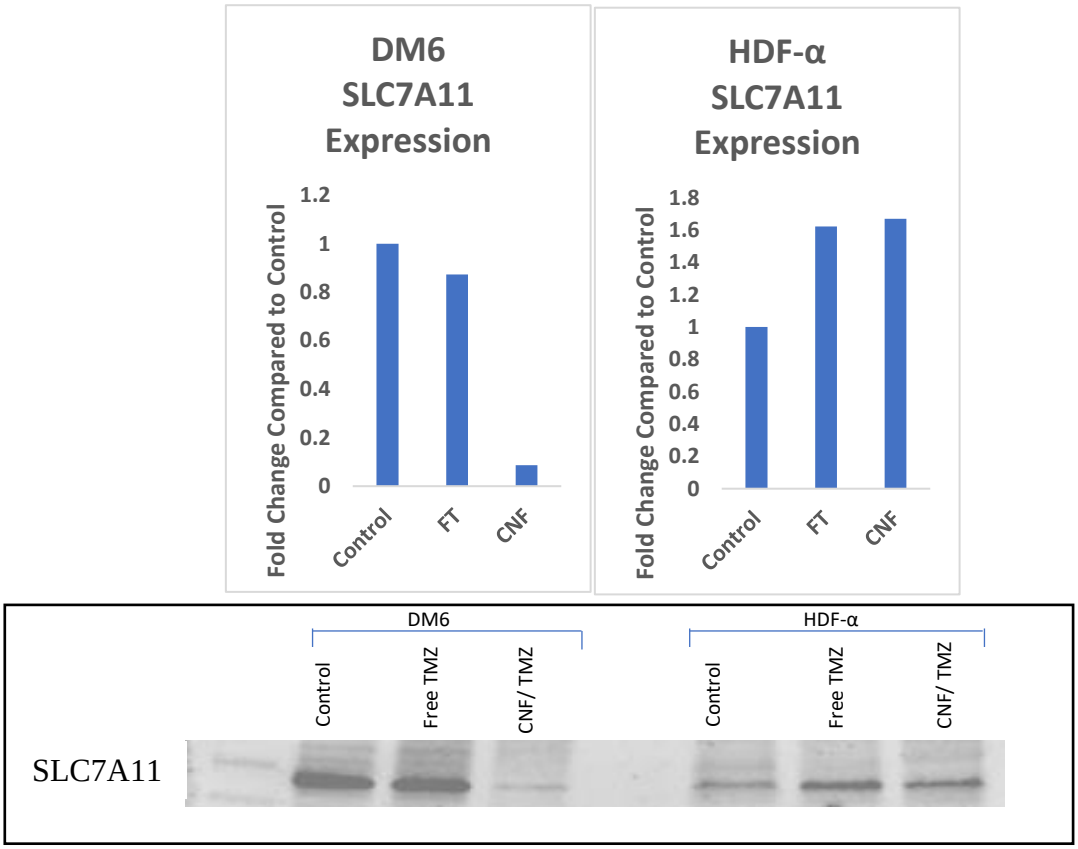

*Figure 36: **SlC7A11 Expression:** Expression of SLC7A11 was highly reduced in DM6 treated with CNF/TMZ indicating a reduced ability to import cystine, required for GSH synthesis. HDF-α showed an increased expression in both treatment groups.*

4.3.10 **Cystathionine Western Blot**

Depletion of Cystathionine would prohibit one of the alternative methods of gaining cysteine for GSH synthesis. Cystathionine is broken down in order for endogenous cysteine production to occur. Depleted levels would result in an ability to contribute to the cysteine pool by endogenous means. I saw a significant decrease that appears to be related to the decrease we saw with Nrf2, as Nrf 2 is the primary transcriptional factor for cystathionine.

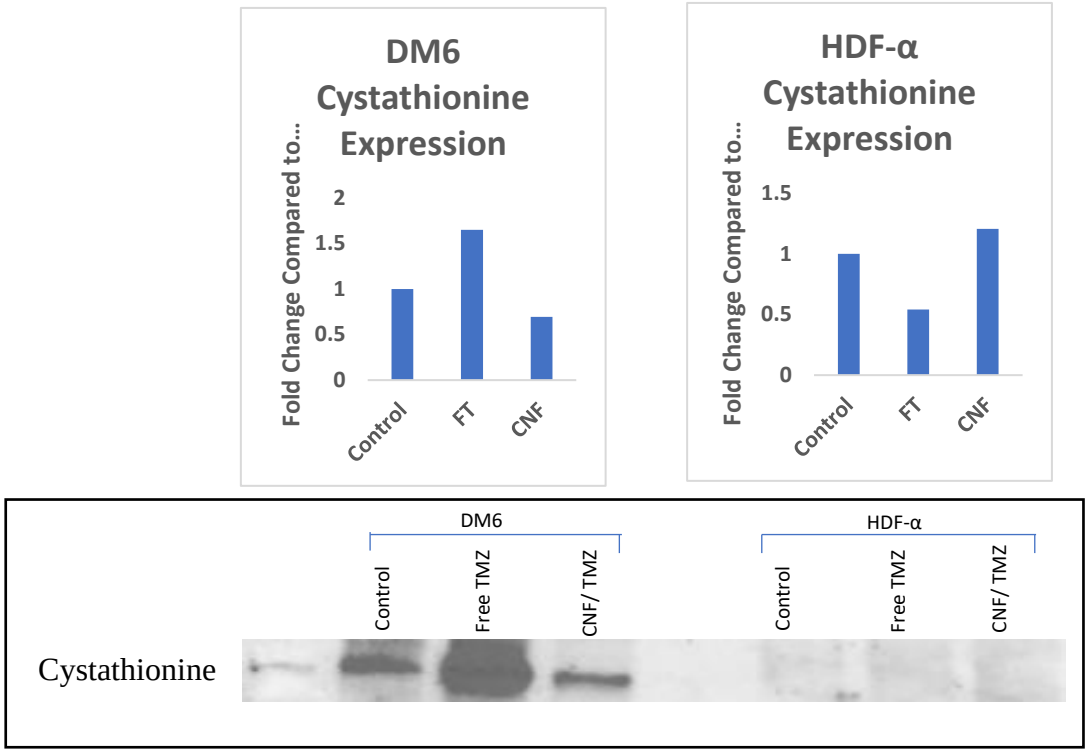

Figure 37: ***Cystathionine Expression:*** *Expression levels of Cystathionine in DM6 treated with CNF/TMZ, while upregulation occurred with treatment of free TMZ. We also saw upregulation of expression in HDF-α cell when treated with CNF/TMZ and downregulation due to free TMZ treatment.*

4.4 Summary

Our results demonstrate some differences between DM6 and HDF-α treatment groups that narrow down the method of cell death our hydrogel uses. DM6 treated with CNF/TMZ show an upregulation of ROS along with a decrease in both total GSH and GSH/GSSG ratio. This is an ideal combination for cells to experience lethal levels of oxidative stress. DM6 treated with Erastin and BSO show a decrease in GSH, yet no increase in ROS, and on their own do does not cause significant cell death. Erastin on its own limits the amount of exogenous cystine that can be up taken by inhibiting activity of SLC7A11 anti-porter in order to create cysteine, yet there is no increase in ROS or cell death, potentially indicating another method of cysteine production that is occurring. The Transsulfuration pathway allows cells to produce endogenous cysteine that is then utilized for GSH production. As Erastin treatment does not also include increased ROS levels, it is possible that the Transsulfuration pathway provides adequate cysteine to

maintain GSH levels to prevent lethal levels of oxidative stress from being reached. BSO puts a hard stop on GSH synthesis, but like Erastin, it does not show increased ROS or cell death, so it seems that BSO on its own does not cause increased oxidative stress to the point of lethality. Both cell lines exhibit decreased levels of MGMT in their respective treatment group to promotes the highest cell death. This is a good indication that CNF/TMZ is able to deplete MGMT reserves in DM6 cells but does not have any impact on MGMT expression in HDF-α, unless treated with FT where MGMT in the drastically reduced, preventing the primary repair body of TMZ DNA damage to be available. CNF/TMZ treatment on DM6 appears to attack on multiple flanks, its main goal being DNA methylation leading to double-stranded breaks (DSB) while also capable of depleting key transcriptional factors such as Nrf2, cascading downwards to reduce SLC7A11 and Cystathionine expression. This multi-way depletion attacks key mechanisms that allow for GSH synthesis. Reiterating the increase in ROS to DM6 when treated with CNF/TMZ, while FT saw no significant increase, and combing that with depletion of GSH via multiple routes creates a perfect storm for lethal oxidative stress. In summary, it appears DM6 cells are able to resist a single attack of having GSH depleted without any ROS increase, as seen with Erastin and BSO treatment. Treatment using CNF/TMZ on DM6 utilizes a multi-prong approach where DNA damage is caused, depleting the primary mechanisms of repair, MGMT, increase ROS possibly through mitochondrial DNA damage while depleting the necessary transcription factor and supporting proteins for GSH synthesis, removing the very important antioxidant from the equation. Ultimately allowing cell death to occur in a high resistant melanoma cell line, while minimizing cell death in normal cells commonly seen within the tumor microenvironment.

Chapter 5:

5.1 Future Direction

Further studies would provide benefits to our understanding of the mechanisms as to how our hydrogel formulation provides its benefit of protection for pH sensitive drugs, proper treatment protocol, and increased understanding of its mechanism of overcoming chemoresistance in malignant cutaneous melanoma. The future direction of this project can be divided into 3 sections: hydrogel characteristics, increased dosage studies, and further molecular studies.

The addition of PAA to our cellulose-based hydrogel is expected to provide amine bonds and a hydrophobic exterior that retains the internal pH of the hydrate, meaning that TMZ dissolved into a hydrate of pH ~5 will be retained in its pro-drug form when loaded into the hydrogel. To correlate these amine bonds to TMZ release we can perform FTIR on the hydrogel at time points related to our release study. Assuming there is a correlation I would expect the amine bond signal to decrease over time as the drug is released. We can measure degradation of the hydrogel, which is traditionally related to drug release, by measuring weight of remaining hydrogel at planned time points. This could prove to be slightly difficult and might require some adjustments as our hydrogel is not crosslinked, meaning it is more vulnerable to degradation and delicate to manipulation to get a measurement. One consideration is the viscosity of our hydrogel, as viscosity could immobilize the TMZ within the nano-network of fibers, reducing gradient mediated release. This can be done by measuring the viscosity using a rotational rheometer.

In our cell viability studies we see cells remaining in our CNF/TMZ group after 48 hours. Are these cells remaining due to inherent or acquired resistance to TMZ or are they remaining because the cytotoxic effect of our treatment is relatively short lasting, and a repeat of the treatment could kill off the remaining cells. Based on the release data and the half-life of TMZ I suspect that the peak cytotoxic effect of TMZ is within 8-16 hours and is severely reduced to a point where cells are not affected out to 48 hours. I think an experiment where a group was added where the original treatment is removed and replaced with an additional treatment at 24 hours, then measuring cell viability at 48 hours. Acquired resistance is more unlikely than inherent resistance as acquired resistance typically requires numerous administrations of the drug, allowing the cells to adapt over a prolonged time.

Our lab has developed a device to create an in vitro invasion assay by coculturing cancer cells surrounded by normal cells, recreating a basic 2D tumor microenvironment. A tumor microenvironment is dynamic, where at various stages of cancer development the normal cells can act as either anti- or pro-tumorigenesis, either increasing or decreasing the efficacy of treatment. Our device allows cells to share the same environment, while being maintaining distinct colonies for evaluation. Further, because we are able to control the initial spacing between the cell types, we can determine whether our treatment has any affect on migration of normal cells, this could be beneficial in the context of wound healing.

Further analysis of the molecular procedures that are used for overcoming chemoresistance can provide a more in-depth picture. Reducing Nrf2 expression or its activity seems a priority in overcoming TMZ resistance, as we see great depletion of protein expression in our CNF/TMZ group where we also see significant cell death. Determining whether the mechanism imposed on Nrf2 is its depletion due to ubiquitination or its inability to translocate into the nucleus to

function as a proper transcription factor or whether the effect is on Nrf2 mRNA expression can more precisely identify the target of our treatment. This can be accomplished using RT-PCR to analyze mRNA levels.

To better confirm the cause of oxidative stress, whether it is primarily due to GSH depletion or an increase in ROS production, quantitative analysis of mitochondrial ROS production could be performed. As the mitochondria is the primary means of ROS production and there is documentation of TMZ acting on mitochondrial DNA, then it is possible that damage to mitochondrial DNA is actively increasing ROS production. Mitochondrial DNA damage can be measured using commercially available assay kits. Targeting ROS within the mitochondria is difficult but there are methods to quantify ROS in a specific region. One method is to use a mitochondrial permeable probe such as Mitotracker CMXH2Ros that gets sequestered within mitochondria and only measures ROS within. You can accompany this with a cytoplasmic fluorescent probe of a different wavelength for cytoplasm ROS quantification. For increased accuracy a cytoplasmic ROS scavenger could be utilized.

For a more global understanding of protein expression quantitative proteomics can be a powerful took for better understanding which pathways are acting in a chemoresistant fashion. This can be an expensive endeavor, but the information gained is difficult to come by from any other method as efficiently. Control groups can be analyzed as a baseline for the protein profile of proliferating DM6 cells, and the same for cells treated with free TMZ to determine which pathways are upregulated to develop chemoresistance, and finally for DM6 cells treated with CNF/TMZ to expose the pathways that are bypassed or altered to allow for cell death to occur. The same setup can be done for the HDF-α cells to make a comparison and determine whether there are specific pathways that can be targeted to treat cancer without harming healthy cells.

5.2 Conclusion

Melanoma has historically been a devastating cancer and incredibly difficult to treat once metastasis has started, and unfortunately this has continued to the present day, with the gold standard of chemotherapy agents, Dacarbazine, only having an overall survival rate of about 22% [24]. Early detection and thorough treatment of melanoma in the early stages before it has migrated away from the skin dramatically increases the survival to near 95%, depending on the actual stage [95, 96]. Continuous improvement in early-stage treatment that is accessible to all populations is still needed. Localized treatments are shown to be more efficient in terms of lower drug concentrations and less off-target cytotoxicity [97-99].Our group developed and tested a cellulose-based hydrogel modified through the addition of polyacrylic acid (PAA) to provide stability to the pH dependent chemotherapy drug TMZ, which would then be released into the tumor microenvironment and degrade into its active components (Figure 1). The aim was to develop a slow releasing vehicle that would reduce cell viability of chemoresistant melanoma cells, while more importantly not significantly harming normal cells seen within the skin and melanoma tumor microenvironment.

The paradigm of maximizing cancer cell death through the administration of a maximal dosage of chemotherapy drug has begun to come under contention. Systemic therapies produce less drug at the site of the tumor, high accumulation in healthy tissue, and often result in a more aggressive phenotype upon resurgence of the tumor [100, 101]. This aggressive phenotype also demonstrates a high resistance to the chemotherapy, which means a higher dosage is required which can result in more serious side effects, the need to add additional treatments causing increase cost and new side effects, or treatment cannot continue resulting ultimately in patient death. New regimens are being evaluated using different dosing and concentration patterns.

Metronomic chemotherapy following an initial high dosage has shown to be more beneficial in stabilizing tumors in terms of size and reducing metastatic behavior [102, 103]. High dose treatments are thought to promote an imbalance between resistant and non-resistant cancer cells within the tumor, which when balanced allow the latter to control the proliferation of the former through competition for nutrients in the fixed space of the tumor. Cells with the machinery for resistance require higher energy requirements and can be contained when their ability to garner nutrients is minimized. By selectively eliminating the non-resistance cells this creates unopposed proliferation of cancer cells resistant to the chemotherapy drug, known as competitive release. The goal should be to maintain a balance within the tumor to contain the more aggressive cells and prevent metastasis or future remission. MDA-MB-231 breast cancer cells were treated with a conventional high dose treatment of paclitaxel, a constantly lowering but repeated dosage, and a dose-skipping protocol in orthotopic mouse xenografts. The treatment involving lowering continuous dosages caused tumor size stabilization and earlier control over tumor growth compared to either standard high dose treatment or skipping-dosages. Low repeated dosages over time also allowed for a cumulatively higher amount of drug to be used compared to the other two regimens [43].

We believe that our data has laid a good foundation for a potential treatment that can be utilized in various ways for the treatment of melanoma. By modifying CNF to a 10% CNF, we were able to effectively reduce cell viability amongst a highly metastatic and chemoresistance melanoma cell line using the pH dependent drug Temozolomide. The degree to which we were able to reduce cell viability was significantly higher than free TMZ at all concentrations, with a large disparity at a concentration of 100uM. Effectively we were able reduce the concentration needed to get more effective results using our 10% CNF. Just as important we significantly

reduced cytotoxicity to HDF-a, a cell common within the skin and tumor microenvironment. The goal of any chemotherapy drug should be to reduce cell viability of the targeted cancer cells, but along with that it is vital to prevent off-target cytotoxic events on normal cells in the vicinity and our 10% CNF proved capable of accomplishing this task utilizing the FDA approved drug, TMZ. Further we were able to show that slow release of TMZ, rather than bulk delivery, was not only able to cause the traditional DNA damage and deplete MGMT but was also able to interfere in GSH synthesis through multiple mechanisms. Our treatment increased ROS levels and decreased GSH levels and GSH/GSSG ratio, indicative of a high oxidative stress environment. Proteins associated with GSH synthesis were also shown to be depleted. Nrf2, a key transcriptional factor for several GSH synthesis related genes was markedly reduced by CNF/TMZ treatment relative to free TMZ delivery. SLC7A11, an antiporter responsible for importing exogenous cystine that is then modified into cysteine for GSH synthesis was also downregulated, likely due to an initial depletion of Nrf2, as Nrf2 strongly regulates SLC7A11 expression. With exogenous cystine import made defective the cells would need to rely on endogenous means to create cysteine, one of which is the Transsulfuration pathway. A key protein in this pathway is cystathionine, which is broken down into several components, one being cysteine. The enzyme cystathionin β-synthase that is responsible for the breakdown of cystathionine is transcriptionally regulated by Nrf2, meaning a depletion of Nrf2 is likely to cause a disturbance in the breakdown of cystathionine and the production of endogenous cysteine. Further interference of GSH pro-tumor activity comes from a minor depletion of GST in DM6 cells, but there was a major upregulation in HDF-ά, possibly acting as a means of resistance allowing the HDF-ά to utilize GST as a catalyst for binding GSH to the TMZ molecules and inactivating their cytotoxic effects. As GST was only mildly downregulated in

CNF/TMZ treated DM6 relative to the other molecules associated with GSH synthesis and activity, binding of GSH to TMZ is likely not as potent of a role in cell death as depletion of GSH through induction of ROS and blockage of cysteine from being produced and imported.

While surgery is still the primary curative process for primary melanoma at early stages, adjuvant and neoadjuvant therapies are highly useful. As an adjuvant therapy our 10% CNF hydrogel could be administered to the resected area to provide further treatment to areas where melanoma cells could still reside as single or very small clusters. These could be cells that were missed during surgical recession or cells that had migrated from the primary tumor and set small satellite lesions under the skin. There are cases where shrinkage of the tumor prior to surgical resection is required or desired, an example being for melanomas on the face where aesthetics needs to be considered. Our hydrogel could be administered as a topical agent to reduce the overall area of the primary tumor prior to surgery, therefore acting as a neo-adjuvant therapy. In cases where the patient is not a candidate for surgery, especially in the elderly, we believe our hydrogel could be administered via intratumoral injection. Finally, as our hydrogel shows the ability to protect acidic pH sensitive drugs it is likely that other drug candidates like TMZ could be loaded into our hydrogel and administered as needed. In concurrence with outside data the protective ability and slow release of TMZ from our 10% CNF hydrogel could promote tumor stabilization without aggravating further proliferation and metastasis of primary melanoma, while conserving healthy tissue in the vicinity of the treatment area. We also elaborated on the means by which slow release of TMZ is able to promote cell death in DM6, without being overly devastating to HDF-ά. It appears to be a mixture of DNA repair protein depletion, namely MGMT, and increased ROS production and depleted GSH synthesis. Likely through a combination of ROS elevation and inhibition of proteins responsible for regulating GSH

synthesis and access to important amino acids like cysteine, starting with Nrf2 depletion, and likely followed by SLC7A11 and Cystathionine depletion, which rely on Nrf2 transcriptional activity directly and indirectly, respectively. We also saw that CNF/TMZ treatment on HDF-ά increased levels of GST which would act as a defense to TMZ by promoting binding of thiol groups on GSH to the highly reactive alkylating agent, detoxifying it. Along with that we failed to see the same level of protein depletion with HDF-ά that we saw with DM6 when treated with CNF/TMZ. It is possible that the upregulation of GST seen in HDF-ά allows for optimal defense to prevent significant damage.

Treating cancer is easy but treating cancer without causing further harm to the patient is the hard part. Treatments need to be both highly effective in killing cancer cells, while minimizing lethal reactions to healthy tissues. It is also important to consider the method of delivery for the treatment as a change in delivery could overcome resistance seen in more traditional methods, improving the long-term benefits of the treatment. Targeted and slow-release vehicles are consistently showing improved responses to treatment over traditional systemic delivery methods, and out research contributes to that knowledge base, along with insight into the mechanisms by which slow-release vehicles can overcome chemoresistance in cutaneous malignant melanoma.

Chapter 6: References

1. Organization, I.A.f.R.o.C.W.H. *Cancer Fact Sheets*. Cancer Today 2018; Available from: https://gco.iarc.fr/today/fact-sheets-cancers.
2. Prevention, C.f.D.C.a. *United States Cancer Statistics: Data Visualizations*. 2020; Available from: https://gis.cdc.gov/Cancer/USCS/DataViz.html.
3. National Cancer Institute: Surveillance, E., and End Results Program. *SEER Cancer Stat Facts: Melanoma of the Skin*. Available from: https://seer.cancer.gov/statfacts/html/melan.html.
4. Center, A.C.S.C.S. *Melanoma of the Skin at a Glance*. 2018; Available from: https://cancerstatisticscenter.cancer.org/#!/cancer-site/Melanoma%20of%20the%20skin.
5. Shain, A.H., et al., *The Genetic Evolution of Melanoma from Precursor Lesions.* New England Journal of Medicine, 2015. **373**(20): p. 1926-1936.
6. Network, T., *Genomic Classification of Cutaneous Melanoma. Cell.* Press.[Google Scholar].
7. Schadendorf, D., et al., *Melanoma.* The Lancet, 2018. **392**(10151): p. 971-984.
8. Galuppini, F., et al., *Tumor mutation burden: from comprehensive mutational screening to the clinic.* Cancer cell international, 2019. **19**: p. 209-209.
9. Alexandrov, L.B., et al., *Signatures of mutational processes in human cancer.* Nature, 2013. **500**(7463): p. 415-421.
10. Hodis, E., et al., *A Landscape of Driver Mutations in Melanoma.* Cell, 2012. **150**(2): p. 251-263.
11. Liu, Y. and M.S. Sheikh, *Melanoma: Molecular Pathogenesis and Therapeutic Management.* Molecular and cellular pharmacology, 2014. **6**(3): p. 228-228.
12. Rhodes, A.R., et al., *Risk Factors for Cutaneous Melanoma: A Practical Method of Recognizing Predisposed Individuals.* JAMA, 1987. **258**(21): p. 3146-3154.
13. Uribe, P., Wistuba, II, and S. González, *BRAF mutation: a frequent event in benign, atypical, and malignant melanocytic lesions of the skin.* Am J Dermatopathol, 2003. **25**(5): p. 365-70.
14. Ballo, M.T., et al., *A critical assessment of adjuvant radiotherapy for inguinal lymph node metastases from melanoma.* Ann Surg Oncol, 2004. **11**(12): p. 1079-84.
15. Stevens, G., et al., *Locally advanced melanoma: results of postoperative hypofractionated radiation therapy.* Cancer, 2000. **88**(1): p. 88-94.
16. Shi, W., *Radiation Therapy for Melanoma*, in *Cutaneous Melanoma: Etiology and Therapy [Internet]*. 2017, Codon Publications.
17. Salama, A.K.S., et al., *Hazard-rate analysis and patterns of recurrence in early stage melanoma: moving towards a rationally designed surveillance strategy.* PloS one, 2013. **8**(3): p. e57665-e57665.
18. *Cutaneous Melanoma: Etiology and Therapy*, in *Cutaneous Melanoma: Etiology and Therapy*, W.H. Ward and J.M. Farma, Editors. 2017, Codon Publications

19. Mrazek, A.A. and C. Chao, *Surviving cutaneous melanoma: a clinical review of follow-up practices, surveillance, and management of recurrence.* The Surgical clinics of North America, 2014. **94**(5): p. 989-viii.
20. Leung, A.M., D.M. Hari, and D.L. Morton, *Surgery for distant melanoma metastasis.* Cancer J, 2012. **18**(2): p. 176-84.
21. Ollila, D.W., *Complete metastasectomy in patients with stage IV metastatic melanoma.* Lancet Oncol, 2006. **7**(11): p. 919-24.
22. Testori, A., et al., *Local and intralesional therapy of in-transit melanoma metastases.* J Surg Oncol, 2011. **104**(4): p. 391-6.
23. Bhatia, S., S.S. Tykodi, and J.A. Thompson, *Treatment of metastatic melanoma: an overview.* Oncology (Williston Park, N.Y.), 2009. **23**(6): p. 488-496.
24. Serrone, L., et al., *Dacarbazine-based chemotherapy for metastatic melanoma: thirty-year experience overview.* J Exp Clin Cancer Res, 2000. **19**(1): p. 21-34.
25. Eggermont, A.M. and J.M. Kirkwood, *Re-evaluating the role of dacarbazine in metastatic melanoma: what have we learned in 30 years?* Eur J Cancer, 2004. **40**(12): p. 1825-36.
26. Quirbt, I., et al., *Temozolomide for the treatment of metastatic melanoma.* Current oncology (Toronto, Ont.), 2007. **14**(1): p. 27-33.
27. Thomas, A., et al., *Temozolomide in the Era of Precision Medicine.* Cancer research, 2017. **77**(4): p. 823-826.
28. Shah, G.D., et al., *Phase II trial of neoadjuvant temozolomide in resectable melanoma patients.* Annals of Oncology, 2010. **21**(8): p. 1718-1722.
29. Middleton, M.R., et al., *Randomized phase III study of temozolomide versus dacarbazine in the treatment of patients with advanced metastatic malignant melanoma.* J Clin Oncol, 2000. **18**(1): p. 158-66.
30. Quirt, I., et al., *Temozolomide for the treatment of metastatic melanoma: a systematic review.* Oncologist, 2007. **12**(9): p. 1114-23.
31. Kiebert, G.M., D.L. Jonas, and M.R. Middleton, *Health-related quality of life in patients with advanced metastatic melanoma: results of a randomized phase III study comparing temozolomide with dacarbazine.* Cancer Invest, 2003. **21**(6): p. 821-9.
32. Wolf, I.H., et al., *Topical Imiquimod in the Treatment of Metastatic Melanoma to Skin.* Archives of Dermatology, 2003. **139**(3): p. 273-276.
33. Park, A.J., et al., *Long-Term Outcomes of Melanoma In Situ Treated With Topical 5% Imiquimod Cream: A Retrospective Review.* Dermatol Surg, 2017. **43**(8): p. 1017-1022.
34. Paul, S.P., *Melanoma Arising after Imiquimod Use.* Case Reports in Medicine, 2014. **2014**: p. 267535.
35. Pasadyn, S.R. and R. Cain, *Topical Imiquimod Induces Severe Weakness and Myalgias After Three Applications: A Case Report.* The Journal of clinical and aesthetic dermatology, 2019. **12**(6): p. 58-59.
36. Larkin, J., et al., *Combined Vemurafenib and Cobimetinib in BRAF-Mutated Melanoma.* New England Journal of Medicine, 2014. **371**(20): p. 1867-1876.
37. Robert, C., et al., *Improved Overall Survival in Melanoma with Combined Dabrafenib and Trametinib.* New England Journal of Medicine, 2014. **372**(1): p. 30-39.

38. Curtin, J.A., et al., *Distinct Sets of Genetic Alterations in Melanoma.* New England Journal of Medicine, 2005. **353**(20): p. 2135-2147.
39. Haluska, F.G., et al., *Genetic alterations in signaling pathways in melanoma.* Clinical cancer research, 2006. **12**(7): p. 2301s-2307s.
40. Wong, D.J.L. and A. Ribas, *Targeted Therapy for Melanoma*, in *Melanoma*, H.L. Kaufman and J.M. Mehnert, Editors. 2016, Springer International Publishing: Cham. p. 251-262.
41. Grzywa, T.M., W. Paskal, and P.K. Włodarski, *Intratumor and Intertumor Heterogeneity in Melanoma.* Translational oncology, 2017. **10**(6): p. 956-975.
42. Kalal, B.S., D. Upadhya, and V.R. Pai, *Chemotherapy Resistance Mechanisms in Advanced Skin Cancer.* Oncology reviews, 2017. **11**(1): p. 326-326.
43. Enriquez-Navas, P.M., et al., *Exploiting evolutionary principles to prolong tumor control in preclinical models of breast cancer.* Science Translational Medicine, 2016. **8**(327): p. 327ra24.
44. Tawbi, H.A. and S.C. Buch, *Chemotherapy resistance abrogation in metastatic melanoma.* Clin Adv Hematol Oncol, 2010. **8**(4): p. 259-66.
45. Zhang, J., M.F. Stevens, and T.D. Bradshaw, *Temozolomide: mechanisms of action, repair and resistance.* Curr Mol Pharmacol, 2012. **5**(1): p. 102-14.
46. Naumann, S.C., et al., *Temozolomide- and fotemustine-induced apoptosis in human malignant melanoma cells: response related to MGMT, MMR, DSBs, and p53.* British journal of cancer, 2009. **100**(2): p. 322-333.
47. Gamcsik, M.P., et al., *Glutathione levels in human tumors.* Biomarkers : biochemical indicators of exposure, response, and susceptibility to chemicals, 2012. **17**(8): p. 671-691.
48. Fan, D.-y., Y. Tian, and Z.-j. Liu, *Injectable Hydrogels for Localized Cancer Therapy.* Frontiers in Chemistry, 2019. **7**(675).
49. Jiang, T., et al., *Enhanced Transdermal Drug Delivery by Transfersome-Embedded Oligopeptide Hydrogel for Topical Chemotherapy of Melanoma.* ACS Nano, 2018. **12**(10): p. 9693-9701.
50. Shoshan, M.C. and S. Linder, *Target specificity and off-target effects as determinants of cancer drug efficacy.* Expert Opin Drug Metab Toxicol, 2008. **4**(3): p. 273-80.
51. Lv, D., et al., *Three-dimensional cell culture: A powerful tool in tumor research and drug discovery.* Oncology letters, 2017. **14**(6): p. 6999-7010.
52. Wilson, M.A. and L.M. Schuchter, *Chemotherapy for Melanoma*, in *Melanoma*, H.L. Kaufman and J.M. Mehnert, Editors. 2016, Springer International Publishing: Cham. p. 209-229.
53. Rizzo, F. and N.S. Kehr, *Recent Advances in Injectable Hydrogels for Controlled and Local Drug Delivery.* Advanced healthcare materials, 2020: p. e2001341.
54. Peppas, N.A., et al., *Hydrogels in Biology and Medicine: From Molecular Principles to Bionanotechnology.* Advanced Materials, 2006. **18**(11): p. 1345-1360.
55. Fan, D.-Y., Y. Tian, and Z.-J. Liu, *Injectable Hydrogels for Localized Cancer Therapy.* Frontiers in chemistry, 2019. **7**: p. 675-675.

56. Elias, P.Z., et al., *A functionalized, injectable hydrogel for localized drug delivery with tunable thermosensitivity: synthesis and characterization of physical and toxicological properties.* J Control Release, 2015. **208**: p. 76-84.
57. Vishnubhakthula, S., R. Elupula, and E.F. Durán-Lara, *Recent Advances in Hydrogel-Based Drug Delivery for Melanoma Cancer Therapy: A Mini Review.* Journal of Drug Delivery, 2017. **2017**: p. 7275985.
58. Redpath, M., et al., *Ibuprofen and hydrogel-released ibuprofen in the reduction of inflammation-induced migration in melanoma cells.* Br J Dermatol, 2009. **161**(1): p. 25-33.
59. Tripathi, S., et al., *A Review on Biocompatible Hydrogel: Formulation Aspect and Evaluation.* Research Journal of Pharmaceutical Dosage Forms and Technology, 2018. **10**: p. 119-122.
60. Kabir, S.M.F., et al., *Cellulose-based hydrogel materials: chemistry, properties and their prospective applications.* Progress in Biomaterials, 2018. **7**(3): p. 153-174.
61. Wada-Ohno, M., T. Ito, and M. Furue, *Adjuvant Therapy for Melanoma.* Curr Treat Options Oncol, 2019. **20**(8): p. 63.
62. Testori, A.A.E., S. Chiellino, and A.C.J. van Akkooi, *Adjuvant Therapy for Melanoma: Past, Current, and Future Developments.* Cancers, 2020. **12**(7): p. 1994.
63. Benya, P.D. and J.D. Shaffer, *Dedifferentiated chondrocytes reexpress the differentiated collagen phenotype when cultured in agarose gels.* Cell, 1982. **30**(1): p. 215-24.
64. Baharvand, H., et al., *Differentiation of human embryonic stem cells into hepatocytes in 2D and 3D culture systems in vitro.* Int J Dev Biol, 2006. **50**(7): p. 645-52.
65. Jeong, Y.M., et al., *3D-Printed Collagen Scaffolds Promote Maintenance of Cryopreserved Patients-Derived Melanoma Explants.* Cells, 2021. **10**(3).
66. Jiang, M., et al., *Targeting ferroptosis for cancer therapy: exploring novel strategies from its mechanisms and role in cancers.* Translational Lung Cancer Research, 2020. **9**(4): p. 1569-1584.
67. Zhao, Y., et al., *The Role of Erastin in Ferroptosis and Its Prospects in Cancer Therapy.* Onco Targets Ther, 2020. **13**: p. 5429-5441.
68. Sui, X., et al., *RSL3 Drives Ferroptosis Through GPX4 Inactivation and ROS Production in Colorectal Cancer.* Frontiers in Pharmacology, 2018. **9**(1371).
69. Zilka, O., et al., *On the Mechanism of Cytoprotection by Ferrostatin-1 and Liproxstatin-1 and the Role of Lipid Peroxidation in Ferroptotic Cell Death.* ACS Central Science, 2017. **3**(3): p. 232-243.
70. Umemura, M., et al., *The iron chelating agent, deferoxamine detoxifies Fe(Salen)-induced cytotoxicity.* Journal of Pharmacological Sciences, 2017. **134**(4): p. 203-210.
71. Eberle, J., et al., *Overcoming apoptosis deficiency of melanoma-hope for new therapeutic approaches.* Drug Resist Updat, 2007. **10**(6): p. 218-34.
72. Li, X., et al., *The Caspase Inhibitor Z-VAD-FMK Alleviates Endotoxic Shock via Inducing Macrophages Necroptosis and Promoting MDSCs-Mediated Inhibition of Macrophages Activation.* Frontiers in Immunology, 2019. **10**(1824).
73. Hileman, E.O., et al., *Intrinsic oxidative stress in cancer cells: a biochemical basis for therapeutic selectivity.* Cancer Chemother Pharmacol, 2004. **53**(3): p. 209-19.

74. Drew, R. and J.O. Miners, *The effects of buthionine sulphoximine (BSO) on glutathione depletion and xenobiotic biotransformation.* Biochem Pharmacol, 1984. **33**(19): p. 2989-94.
75. Meierjohann, S., *Oxidative stress in melanocyte senescence and melanoma transformation.* Eur J Cell Biol, 2014. **93**(1-2): p. 36-41.
76. Liu-Smith, F., R. Dellinger, and F.L. Meyskens, Jr., *Updates of reactive oxygen species in melanoma etiology and progression.* Archives of biochemistry and biophysics, 2014. **563**: p. 51-55.
77. Pendyala, L., et al., *Effect of glutathione depletion on the cytotoxicity of cisplatin and iproplatin in a human melanoma cell line.* Cancer Chemother Pharmacol, 1997. **40**(1): p. 38-44.
78. Braidy, N., et al., *The Precursor to Glutathione (GSH), γ-Glutamylcysteine (GGC), Can Ameliorate Oxidative Damage and Neuroinflammation Induced by Aβ40 Oligomers in Human Astrocytes.* Frontiers in Aging Neuroscience, 2019. **11**(177).
79. Gregg, X.T. and J.T. Prchal, *Chapter 44 - Red Blood Cell Enzymopathies*, in *Hematology (Seventh Edition)*, R. Hoffman, et al., Editors. 2018, Elsevier. p. 616-625.
80. Wang, Z., et al., *Ferroptosis suppressed the growth of melanoma that may be related to DNA damage.* Dermatologic Therapy, 2019. **32**(4): p. e12921.
81. Kennedy, L., et al., *Role of Glutathione in Cancer: From Mechanisms to Therapies.* Biomolecules, 2020. **10**(10).
82. Cen, D., et al., *Disulfiram facilitates intracellular Cu uptake and induces apoptosis in human melanoma cells.* Journal of medicinal chemistry, 2004. **47**(27): p. 6914-6920.
83. Yu, W., et al., *O6-Methylguanine-DNA Methyltransferase (MGMT): Challenges and New Opportunities in Glioma Chemotherapy.* Frontiers in Oncology, 2020. **9**(1547).
84. Niture, S.K., et al., *Increased expression of the MGMT repair protein mediated by cysteine prodrugs and chemopreventative natural products in human lymphocytes and tumor cell lines.* Carcinogenesis, 2007. **28**(2): p. 378-389.
85. Kim, K.M. and S.H. Ki, *Chapter 28 - Nrf2: A Key Regulator of Redox Signaling in Liver Diseases*, in *Liver Pathophysiology*, P. Muriel, Editor. 2017, Academic Press: Boston. p. 355-374.
86. Steele, M.L., et al., *Effect of Nrf2 activators on release of glutathione, cysteinylglycine and homocysteine by human U373 astroglial cells.* Redox biology, 2013. **1**(1): p. 441-445.
87. McLellan, L.I. and C.R. Wolf, *Glutathione and glutathione-dependent enzymes in cancer drug resistance.* Drug Resistance Updates, 1999. **2**(3): p. 153-164.
88. Nguyen, C., et al., *NRF2-regulated genes SLC7A11 and NQO1 confer chemoresistance in mesotheliomas.* Cancer Research, 2008. **68**(9 Supplement): p. 3250.
89. Galván, I., et al., *High SLC7A11 expression in normal skin of melanoma patients.* Cancer Epidemiol, 2019. **62**: p. 101582.
90. Sato, M., et al., *Loss of the cystine/glutamate antiporter in melanoma abrogates tumor metastasis and markedly increases survival rates of mice.* Int J Cancer, 2020. **147**(11): p. 3224-3235.
91. Ripps, H. and W. Shen, *Review: taurine: a "very essential" amino acid.* Molecular vision, 2012. **18**: p. 2673-2686.

92. Jhee, K.H. and W.D. Kruger, *The role of cystathionine beta-synthase in homocysteine metabolism.* Antioxid Redox Signal, 2005. **7**(5-6): p. 813-22.
93. Liu, N., X. Lin, and C. Huang, *Activation of the reverse transsulfuration pathway through NRF2/CBS confers erastin-induced ferroptosis resistance.* Br J Cancer, 2020. **122**(2): p. 279-292.
94. Rosado, J.O., M. Salvador, and D. Bonatto, *Importance of the trans-sulfuration pathway in cancer prevention and promotion.* Mol Cell Biochem, 2007. **301**(1-2): p. 1-12.
95. Davis, L.E., S.C. Shalin, and A.J. Tackett, *Current state of melanoma diagnosis and treatment.* Cancer Biol Ther, 2019. **20**(11): p. 1366-1379.
96. Quintanilla-Dieck, M.J. and C.K. Bichakjian, *Management of Early-Stage Melanoma.* Facial Plast Surg Clin North Am, 2019. **27**(1): p. 35-42.
97. Norouzi, M., B. Nazari, and D.W. Miller, *Injectable hydrogel-based drug delivery systems for local cancer therapy.* Drug Discov Today, 2016. **21**(11): p. 1835-1849.
98. Oliva, N., et al., *Designing Hydrogels for On-Demand Therapy.* Acc Chem Res, 2017. **50**(4): p. 669-679.
99. Fan, D.Y., Y. Tian, and Z.J. Liu, *Injectable Hydrogels for Localized Cancer Therapy.* Front Chem, 2019. **7**: p. 675.
100. Senapati, S., et al., *Controlled drug delivery vehicles for cancer treatment and their performance.* Signal transduction and targeted therapy, 2018. **3**: p. 7-7.
101. Wolinsky, J.B., Y.L. Colson, and M.W. Grinstaff, *Local drug delivery strategies for cancer treatment: gels, nanoparticles, polymeric films, rods, and wafers.* Journal of controlled release : official journal of the Controlled Release Society, 2012. **159**(1): p. 14-26.
102. Satti, J., *The emerging low-dose therapy for advanced cancers.* Dose-response : a publication of International Hormesis Society, 2009. **7**(3): p. 208-220.
103. Maiti, R., *Metronomic chemotherapy.* Journal of pharmacology & pharmacotherapeutics, 2014. **5**(3): p. 186-192.